Session 2: Structural modelling for numerical analysis

Session 2

Structural Modelling for Numerical Analysis

Leere Seite
Blank page
Page vide

Dynamic Finite Element Analysis of Reinforced Concrete Structures

Analyse dynamique de structures en béton armé à l'aide d'éléments finis

Dynamische Finite Elemente Analysis von Stahlbetontragwerken

CHRISTIAN MEYER
Associate Professor
Dpt. of Civil Eng. and Eng. Mechanics, Columbia University
New York, NY, USA

SUMMARY
This report summarizes the current state of the art in finite element and other numerical techniques applied to concrete structures subjected to dynamic loads. The various sources of dynamic loads are identified, followed by a brief statement on strain-rate effects on material properties. The behavior of reinforced concrete members under cyclic loading is discussed, as well as some of the mathematical models devised to sumulate this behavior. The last section considers some of the applicable dynamic analysis methods.

RESUME
Cet article résume l'état actuel des connaissances sur les éléments finis et autres méthodes numériques appliquées aux structures en béton armé soumises à des charges dynamiques. Les différentes origines des charges dynamiques sont établies; un bref exposé des effets de la vitesse de déformation sur les propriétés des matériaux est présenté. Le comportement des poutres en béton armé soumises à un cycle de charges et quelques modèles mathématiques destinés à la simulation du comportement sont discutés. La dernière partie traite quelques méthodes d'analyse dynamique.

ZUSAMMENFASSUNG
Dieser Bericht fasst den heutigen Stand der Finite-Element- und anderer numerischer Methoden zusammen, welche auf dynamisch beanspruchte Stahlbetontragwerke angewendet werden. Die verschiedenen Ursprünge der dynamischen Lasten werden aufgeführt, gefolgt von einer Bemerkung über den Einfluss der Dehnungsgeschwindigkeit auf die Materialeigenschaften. Das Verhalten von Stahlbetonstäben unter zyklischer Belastung wird diskutiert, sowie einige der mathematischen Modelle, welche dieses Verhalten simulieren sollen. Der letzte Abschnitt behandelt einige Anwendungsmethoden für dynamische Analysen.

1. INTRODUCTION

It is the responsibility of the structural engineer to ensure that all structures are accurately analyzed and designed to safely withstand the anticipated loads. Most structures are designed on the basis of relatively simple methods which are the result of mostly empirical research compiled over many decades and which have been confirmed by innumerable experimental tests. This traditional approach to design has generally been adequate because

1. the structures designed by these methods have by and large behaved satisfactorily, and
2. the extraordinary complex behavior of concrete (an inelastic, viscous, inhomogeneous material) has stymied any attempts at rational formulations to serve as foundation for alternate design methods.

On both counts, considerable changes have taken place in recent years.

The adequacy of traditional empirical design methods has been questioned in a number of applications. Foremost is the construction of nuclear power plants. The overall design requirement that the uncontrolled release of radioactivity be prevented at any rate places demands on the structural analyst and designer that cannot be met by the simplified traditional methods.

A second application for which the standard design methods are clearly inadequate is the design of concrete structures to safely withstand earthquake ground motions. The destructiveness of strong earthquakes is the driving force behind the search for advanced methods of analysis and design that are based on thorough understanding of reinforced concrete behavior.

A third class of structures for which the old design methods are not satisfactory can be broadly labeled as defense installations, such as hardened shelters and missile silos. Their unusual loadings and performance requirements set this class of structures apart from all others,

As the above examples illustrate, there is no reason to feel complacent about currently available design methodology--we have to search for new improved methods. Advanced mechanics in reinforced concrete provides the foundation for these methods. Three separate and yet interrelated tasks can be distinguished:

1. to identify the material properties of concrete and steel;
2. to model the behavior of reinforced concrete members;
3. to analyze the structural response of concrete structures.

This report will summarize the current state of the art in finite element and other numerical techniques applied to concrete structures. While the companion introductory report by Argyris et al emphasizes primarily quasi-static loadings, this report will concentrate on the special problems associated with dynamic loads.

After a brief discussion of the different kinds of dynamic loads, the report will be organized along the three tasks mentioned above. First, the dynamic effects of loading rates on the material properties are discussed briefly. Thereafter, the behavior of reinforced concrete members under cyclic loading will be summarized, as well as some of the mathematical models that have been devised in the past for the purpose of simulating this behavior. The last section will consider some analysis methods that are appropriate for the response analysis of concrete structures to dynamic loads.

2. DYNAMIC LOADS

There are few loads that are truly static in nature, although many types of loadings are applied slowly enough not to excite any significant dynamic response. Still, most loadings that are of concern to the designing engineer because of their effect on the safety or serviceability of structures are of dynamic nature. Below follows a summary description of the important dynamic load categories and their main effects on structures.

2.1 Earthquakes

Most earthquakes occur when the stresses in the border regions of tectonic plates exceed the strength of the rock materials and the vast amounts of stored strain energy are suddenly released, radiating by wave propagation through the earth [1]. Often, the earthquake causes ground rupture in the direct vicinity of the causative fault, above the epicentrum. Although such ground rupture zone may extend for hundreds of miles along the fault in a large earthquake, the directly affected area is normally small. Yet, it is next to impossible under economic constraints, to design structures to safely withstand ground rupture.

The much more important effect of an earthquake is the ground shaking that may set hundreds or thousands of square miles in motion. Of this effect, the structural engineer is concerned more with the intensity of ground shaking than with the Richter magnitude, because it is the intensity which is the primary measure of the effect that the earthquake has on the response of structures.

The ground motion effect is equivalent to inertia loads applied to the various mass points of the structure with its base fixed. These inertia loads are equal to the masses multiplied with the ground acceleration time history.

The importance of earthquake loadings for reinforced concrete structures lies in the fact that reinforced concrete members suffer varying degress of stiffness degradation if subjected to cyclic loading into the inelastic range. It is this decrease in stiffness, coupled with severe cracking of the concrete and yielding of flexural and shear reinforcement that poses the main difficulties when analyzing concrete structures subjected to strong earthquake ground motions. There is no evidence, however, that the load-carrying mechanisms are affected appreciably by the dynamic nature of the loads. In other words, provided the effective inertia loads are correctly simulated, equivalent slow-motion load tests should cause similar structure responses. Thus, the reinforced concrete models developed for statically applied loads can be used also for dynamic loads due to earthquakes.

2.2 Wind

Atmospheric disturbances are ubiquitous on earth and therefore all above-ground structures have to be designed to resist the resulting wind loads [2]. These may be associated with rather steady air movements which can be simulated with statically applied equivalent pressures, or they may be caused by buffeting of truly dynamic nature. The intensities vary widely, from those due to moderate gusts, up to those accompanying tornadoes and hurricanes. While earthquake ground accelerations are characterized by vibratory motion about a zero base line, wind can be considered to consist of pressure fluctuations about a static lateral pressure associated with a mean velocity. This decompositon has the advantage that the mean velocity component can be treated as a static load, while the remaining oscillatory component can be analyzed by similar analysis techniques as earthquake effects. When superimposing the two components, attention has to be paid to the nonlinearity of concrete response.

As far as the dynamic effect of wind loading on reinforced concrete is concerned, a statement similar to that on earthquakes can be made: strain rates induced by wind loadings are not high enough to have a marked effect on the response behavior so that any material models can be used for dynamic analysis as if wind loads are applied very slowly, provided, of course, that the inertia effects are duly accounted for.

2.3 Ocean Waves

Ever since the limited world reserve of fossil fuels started to affect entire national economies, the exploration of the seas for oil became an economical necessity and the construction of concrete drilling platforms a reality. The loadings imposed on these structures by the sea are truly remarkable, since some of the richest off-shore oil fields are situated in the most punishing environments on earth. The loadings consist of extraordinary surface wave forces as well as below-surface water currents. The resulting pressures and drag forces that act on the structure have to be included in any analysis and their dynamic effects must be considered for design.

Earthquakes, wind and ocean waves all have in common that the load intensities and frequency contents are highly random quantities. Single deterministic analyses are therefore of only limited value, and the design for unique deterministic loads raises questions about the reliability of the structure in withstanding future events.

2.4 Missile Impact

The problem of missile impact arises in a number of situations in which reinforced concrete walls or roofs serve as protection against missiles such as tornado-borne debris, aircraft impact, industrial missiles such as fragments of a fractured turbine, high-energy pipe ruptures, or against penetrators used in military attack. Such missile barriers are common design features in safety-class structures of nuclear power plant facilities, as well as in hardened military shelters.

For many of these design problems, the empirical methods proposed in the literature are not adequate. More refined numerical simulation techniques are needed to predict the target response. It is the objective of such numerical calculations to determine the depth of penetration or the residual velocity of the missile if penetration occurred, whether concrete fragments come off the front or real surface, or whether a plug forms in the concrete.

At the high missile velocities considered here, concrete properties, especially tensile strength, are strongly strain-rate dependent. Numerical analysis programs designed to simulate missile impact must therefore be general enough to incorporate a most general material model.

2.5 Blast

Blast loads are encountered primarily in the field of weapons effects on protective structures. The predominant effects are caused by airblast or by shock waves propagating through the ground or by a combination of both. Special cases include explosions on the surface of a concrete structure in which the load intensity depends on the mass of the explosive casing and detonation products.

The main effects of airblast are due to dynamic overpressure and reflected pressure. An example of overpressure loading is a surface-flush structure whose roof is exposed to a shock wave propagating in air. An example of reflected pressure loading is an above-ground structure having a dimension

perpendicular to the direction of shock propagation; these are virtually all above-ground structures. The parameters governing the pressure and impulse delivered to the target include the explosive yield, height-of-burst, range of the target from the lowest point, and environmental factors such as atmospheric dust. Although conclusive evidence is lacking, it is generally considered that brittle modes of failure such as shear failures can be explained in terms of peak pressure. In contrast, ductile failure modes such as flexural failure are thought to depend heavily on impulse.

All structures sited within a critical range of an explosion are subjected to ground shock. Attenuation of shock intensity due to geometric dispersion and hysteresis energy absorption is very significant and extremely complicated due to the complexity of in-situ properties of rock and soil. Direct or crater-induced shock begins at or beneath the explosion and propagates as a wave train past the structure. Airblast-induced ground shock is generated when the traveling overpressure pulse loads the ground surface.

2.6 Special Nuclear Power Plant Loadings

In providing for reliable designs of safety-class nuclear power plant structures, a number of special load cases due to various stipulated accident conditions have to be considered and designed for. External and internally generated missiles have already been mentioned. In the case of high energy pipe rupture, the loading of pipe impact on bumpers, snubbers and supports is to be considered as well as the force due to jet impingement, both of which are highly dynamic phenomena. In boiling water reactors, the sudden activation of safety relief valves gives rise to very high pulsating pressures both inside the pressure suppression pool as well as in the containment structure.

2.7 Mechanical Vibrations

Reinforced concrete structures are often designed to house and/or support mechanical equipment or machinery which exerts mostly steady-state harmonic vibrations to the supporting structure. An important and common example are the support frames or pedestals for turbines. The analysis and design for such loads are more straightforward than for the previously discussed dynamic loads, because they are neither as destructive as blast or missile impact, nor are they as unpredictable as earthquakes, wind, or ocean waves. The operating frequencies are usually known to a high degree of certainty, and by carefully tuning the support structure with the operating characteristics of the equipment, resonance amplification in the important natural modes of vibration can be avoided. Since the response to the operating loads is generally linear, advanced numerical techniques such as the finite element method are seldom required to analyze such structures.

3. MATERIAL PROPERTIES

For the dynamic analysis of concrete structures it is important to determine to what extent the material properties are strain-rate dependent. Most laboratory experiments that have been undertaken to investigate the effect of strain rates on the various properties of concrete were conducted at rates similar to those associated with earthquakes, wind and wave loadings. Test results for strain rates of blast or missile impact loading are much sparser [3,4].

The strain-rate effects on the constitutive relations of concrete have been summarized by Taylor [5]. Experiments with the primary objective of studying the strain-rate effect of earthquake loadings have been conducted by Mahin and Bertero [6]. From this study the following conclusions were drawn.

a) Displacement rates showed negligible effect on initial stiffness.

b) High strain rates of the order 0.05 in./in./sec increased the yield strength of reinforced concrete members by more than 20%, but only in the initial excursion into the inelastic range.

c) In subsequent cycles with loads up to the same displacement amplitudes such as in steady-state cycling, differences in either stiffness or strength were rather small.

d) Strain-rate effects on strength diminished with increased excursions into the strain hardening range.

e) No substantial changes were observed in ductility and overall energy absorption capacity.

Otani [7] has observed that strain rates during oscillations are highest at low stress levels and decrease gradually toward a peak strain. Also, cracking and yielding of a reinforced concrete member reduce the stiffness, hence the period of oscillation becomes longer as structural damage increases. Furthermore, such damage is normally caused by a few lower modes of vibration, whose periods are relatively long. For these reasons, the strain-rate effect may not be as important as some material tests under extraordinary high and mostly constant strain rates indicate. Hysteresis loops obtained from dynamic tests of single-story one-bay reinforced concrete frames compared favorably with those obtained from quasi-static tests [8].

4. REINFORCED CONCRETE BEHAVIOR UNDER CYCLIC LOADING

Research in earthquake engineering and concern for the safety of nuclear power plant facilities have been responsible for most of the current knowledge regarding the mechanical behavior of reinforced concrete under static as well as dynamic loads. The findings of these studies can readily be applied to other kinds of dynamic loads as long as the strain rates are of the same order of magnitude. This is the case for both wind and ocean wave loadings. Their different dynamic characteristics have no immediate bearing upon the material properties.

The awesome complexity of reinforced concrete behavior under cyclic loading makes it all but impossible to derive a generally valid mathematical model that can completely include the effects of all parameters involved. Therefore it is advantageous to isolate flexural and shear behavior from bar slip and bond characteristics as well as experimental setups would permit.

4.1 Flexural Behavior

A number of investigators have studied the flexural behavior of reinforced concrete members under cyclic loads in the laboratory [9,10]. Figure 1 shows a typical moment-curvature diagram obtained from a test of a simply supported beam [10]. As can be noticed, the stiffness decreases gradually as a function of load, and under load reversal forms a pronounced hysteresis loop which provides for an appreciable amount of energy absorption. The hysteresis loops remain remarkably stable for a number of load reversals, provided the maximum prior displacement amplitude is not exceeded. The energy which is input into the structure by, for example, an earthquake, can in this case be effectively dissipated without further deterioration or reduction of ultimate strength. A necessary prerequisite for this desirable behavior is a sufficient amount of confinement reinforcement, as it is required by Appendix A of the ACI Building Code [11], or by special design practice [12].

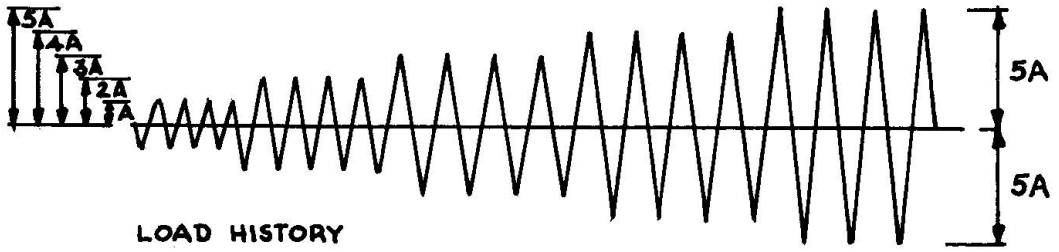

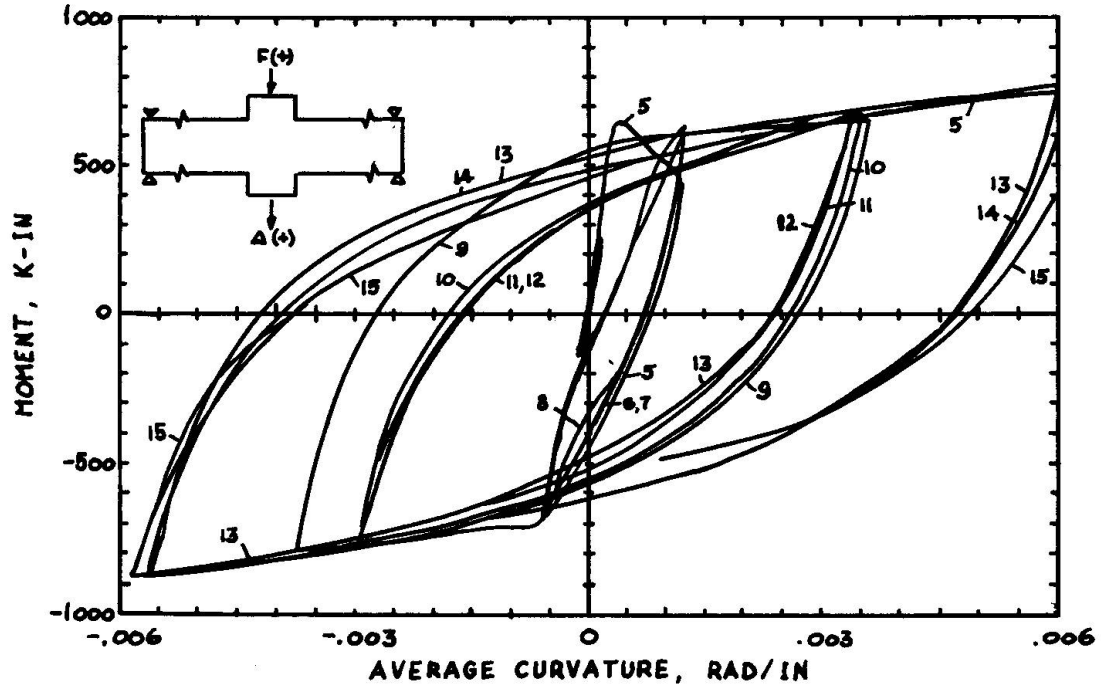

FIG. 1 MOMENT - CURVATURE DIAGRAM (REF. 10)

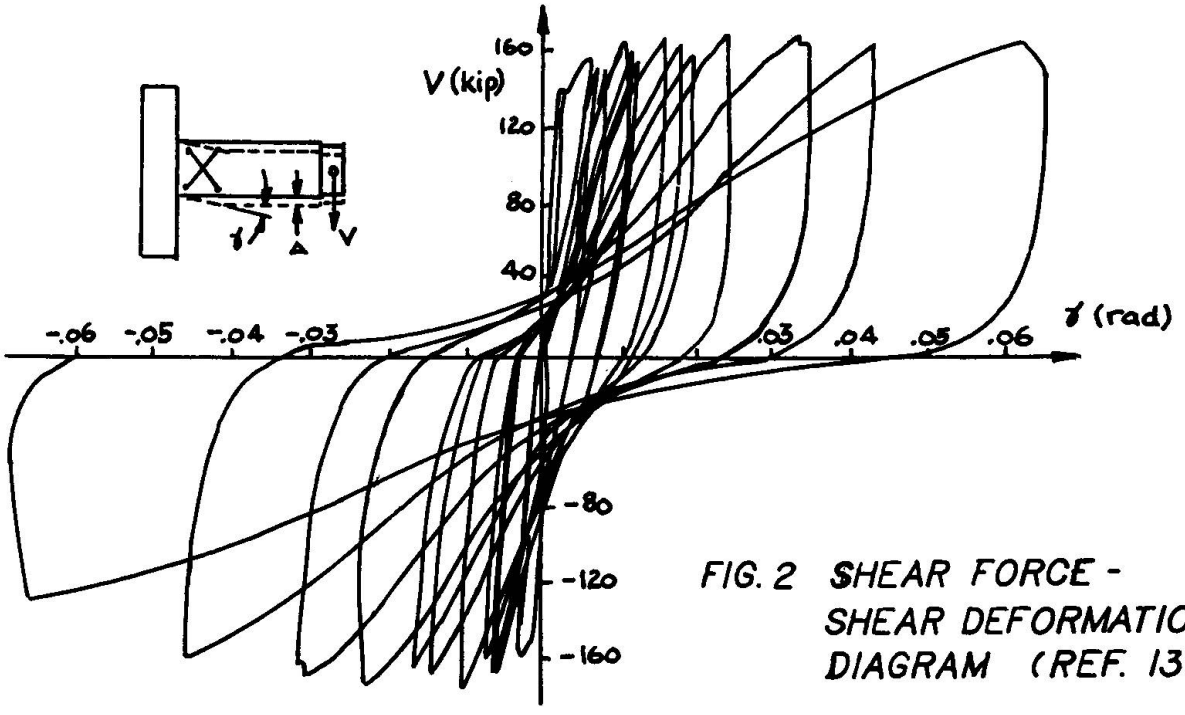

FIG. 2 SHEAR FORCE - SHEAR DEFORMATION DIAGRAM (REF. 13)

In columns, the axial compression tends to decrease the flexural ductility, while delaying the tensile and shear cracking of concrete as well as the yielding of the main reinforcement. The ductility reduction is of most concern to designers; therefore it is good frame design practice to avoid the formation of plastic hinges in columns and to restrict hysteretic energy absorption to the girders.

4.2 Shear Behavior

In order to isolate shear behavior from flexural behavior, relatively short cantilever beams have been tested in the laboratory, and the shear deformations were measured by strain gages arranged in two diagonal and orthogonal directions [13,14]. A typical shear force-shear deformation diagram as shown in Fig. 2 is to some degree reminiscent of the moment-curvature diagram of Fig. 1 [13]. However, it is not an easy matter to completely separate the shear distortions from the other deformation components.

The limited number of experimental data show that in contrast to the flexural stiffness, the shear stiffness typically experiences a gradual increase during loading in either direction, up to an equivalent "yield" level. This behavior gives the shear force-shear deformation hysteresis diagram a "pinched" shape and can be explained as follows. The first complete load cycle far into the inelastic range causes two orthogonal diagonal cracks which reduce the shear stiffness to almost zero for small loads. As the loads in subsequent cycles are increased in either direction, relative slip occurs across the crack until aggregate interlock is activated, which accounts for the sharp increase in apparent shear stiffness.

In contrast to the stable flexural hysteresis behavior, the shear hysteresis loops decay with the number of load reversals, even if the maximum load level is not exceeded. This deterioration is the result of gradual abrasion and cracking of the concrete in the crack region and reduces the energy absorption capacity considerably. This effect of load history on the shear deformation behavior is therefore very important and cannot be neglected when analyzing structures in which the shear behavior has a marked influence on the overall structural response, such as in shear walls, short spandrel beams in coupled shear walls, or in the critical region around the columns in flat plate and flat slab construction.

The shear deformation effect can be modeled in dynamic finite element analysis by either discrete or distributed models. In discrete models, dowel action and aggregate interlock are incorporated by means of special spring elements whose characteristics are determined by experiments. In distributed models, the shear modulus for the elasticity matrix is continually updated in order to simulate the shear behavior.

4.3 Bar Slip and Bond Deterioration

In reinforced concrete frames, beams and columns are normally built integrally so that a certain amount of interaction between adjoining members can be expected. In a typical beam-column assembly such as shown in Fig. 3 [14], for the indicated loading, the right beam moment tends to pull the upper reinforcing bars out of the joint, while the left beam moment helps by pushing. For the bottom reinforcement, both moments are additive in the tendency of pulling the bars to the left. Any kind of cracking in this highly stressed joint region, be it due to flexural or shear action, will only exacerbate the bond deterioration to be expected. The general shape of the moment-bar slip rotation curve is somewhat similar to that of the shear force-shear distortion

diagram of Fig. 2, characertized by pinched hysteresis loops. Once the bars are free to move within the joint zone, the contribution of bar slip to the structure displacements can be significant, especially for stiff members with relatively small flexural and shear deformations.

5. MATHEMATICAL MODELS FOR CONCRETE MEMBERS

It is convenient to classify mathematical models for reinforced concrete members into four categories, according to their degree of complexity and accuracy. The most complex and expensive models have been devised for finite element analysis. These allow quite satisfactory simulation of test results for many different situations [15,16]. The large size of the problems in terms of degrees of freedom and the resulting expense preclude the use of finite element models for general design purposes. Only in exceptional cases such as certain safety-class nucler power plant structures is it conceivable that finite element analyses are directly used for design purposes. In the majority of situations, finite element studies may be used to study the behavior of concrete members and to derive from these studies simplified models for more common design applications. Some of the finite element models that have been presented in the literature will be described briefly below.

On the next lower level of sophistication, the moment-curvature relationships of sections are determined by subdividing the cross-sections into a finite number of layers so that these may be called "semi-finite element" models. The computational effort required to establish complete moment-curvature diagrams for each member in a structure is still so overwhelming that general use for structural analysis is seldom feasible.

In order to reach a balance between computational expense and required accuracy for design purposes, another step of simplification has to be taken which leads to the determination of moment-curvature relationships for an entire member directly. Such models may therefore be termed "member-size" models. They can be used directly to determine the member stiffness properties which are in general time- and displacement-dependent. In order to be accurate, the model should reflect the hysteretic characteristics of the member's flexural, shear and bond behavior well into the inelastic region, if the analysis objective includes strength predictions for the structure under consideration. Several such models have been successfully used in the past and will be included in the discussion below.

Models of the lowest level of complexity can be devised to lump the behavioral characteristics of all beams and columns of one building story together and to replace them by an equivalent beam with properties which somehow approximate the mechanical behavior of the structure. Such models are generally too inaccurate and inadequate for design purposes and will not be covered in this report. They may prove useful for certain kinds of studies in which the relative importance of certain parameters is investigated. The comparably small computational effort permits large ranges for such parameters to be studied.

5.1 Finite Element Models

The generality of the finite element method permits us to directly model discontinuities with the mesh layout; concrete elements and steel elements can be modeled separately, with specialized bond elements simulating the interactive forces. All attention can thereafter be concentrated on the establishment of constitutive material laws which are all by themselves complicated indeed.

One model for finite element analysis is based on so-called equivalent uniaxial strains [17,18]. Consider the incremental constitutive equations for an orthotropic plane stress material

$$\begin{Bmatrix} d\sigma_1 \\ d\sigma_2 \\ d\tau_{12} \end{Bmatrix} = \frac{1}{1-\nu_1\nu_2} \begin{bmatrix} E_1 & \nu_2 E_1 & 0 \\ \nu_1 E_2 & E_2 & 0 \\ 0 & 0 & (1-\nu_1\nu_2)G \end{bmatrix} \begin{Bmatrix} d\varepsilon_1 \\ d\varepsilon_2 \\ d\gamma_{12} \end{Bmatrix} \tag{1}$$

where $\nu_1 E_2 = \nu_2 E_1$ and subscripts 1 and 2 denote the current principal stress axes. With the introduction of an equivalent Poisson's ratio, ν,

$$\nu^2 = \nu_1\nu_2 \tag{2}$$

and the assumption that the shear modulus G is approximately independent of axis orientation, i.e.,

$$(1-\nu^2)\,G = \frac{1}{4}\,(E_1 + E_2 - 2\nu\sqrt{E_1E_2}\,) \tag{3}$$

Eq. 1 takes on the form

$$\begin{Bmatrix} d\sigma_1 \\ d\sigma_2 \\ d\tau_{12} \end{Bmatrix} = \frac{1}{1-\nu^2} \begin{bmatrix} E_1 & \nu\sqrt{E_1E_2} & 0 \\ & E_2 & 0 \\ (\text{symm.}) & & \frac{1}{4}\,(E_1+E_2-2\nu\sqrt{E_1E_2}\,) \end{bmatrix} \begin{Bmatrix} d\varepsilon_1 \\ d\varepsilon_2 \\ d\gamma_{12} \end{Bmatrix} \tag{4}$$

Defining incremental equivalent uniaxial strains as

$$\begin{aligned} d\varepsilon_{1u} &= \frac{1}{1-\nu^2}\left[d\varepsilon_1 + \nu\,\frac{E_2}{E_1}\,d\varepsilon_2\right] \\ d\varepsilon_{2u} &= \frac{1}{1-\nu^2}\left[d\varepsilon_2 + \nu\,\frac{E_1}{E_2}\,d\varepsilon_1\right] \end{aligned} \tag{5}$$

Eq. 4 simplifies further to the form

$$\begin{aligned} d\sigma_1 &= E_1 d\varepsilon_{1u} \\ d\sigma_2 &= E_2 d\varepsilon_{2u} \\ d\tau_{12} &= G\,d\gamma_{12} \end{aligned} \tag{6}$$

which are of the same form as those for uniaxial stress conditions. The integration of Eq. 6 leads to

$$\varepsilon_{iu} = \int \frac{d\sigma_i}{E_i} \qquad i = 1,2 \tag{7}$$

or its discrete equivalent,

$$\varepsilon_{iu} = \sum_{\text{all load increments}} \frac{\Delta\sigma_i}{E_i} \qquad i = 1,2 \tag{8}$$

where $\Delta\sigma_i$ is the incremental change in the principal stress σ_i.

It should be noted that the ε_{iu} are not real strains; they do not transform under coordinate transformations as real strains do. Further, they are accumulated in the principal stress directions which in general change during loading, so that ε_{1u} for example does not provide a deformation history in a fixed direction, but rather in the continuously changing direction corresponding to principal stress σ_1. Nevertheless, these quantities make it possible to use quite realistic hysteresis rules for plain concrete. The basic idea is that once the stress-strain law has been written in a form similar to that for the uniaxial case, stress-strain curves similar to the uniaxial stress-strain response can be used.

Another, quite different model is based on endochronic theory [19,20] and has been shown to describe very well the response of plain concrete under cyclic loads and also under multiaxial stress. It consists of characterizing the inelastic strain accumulation by a scalar intrinsic time parameter whose increment is a function of strain increments. Thus the form of the endochronic constitutive law for short time deformations of concrete is independent of time,

$$de_{ij} = \frac{ds_{ij}}{2G} + de''_{ij}, \quad de''_{ij} = \frac{s_{ij}}{2G}\frac{d\zeta}{Z_1}, \quad d\varepsilon = \frac{d\sigma}{3K} + d\lambda \tag{9}$$

in which $e_{ij} = \varepsilon_{ij} - \delta_{ij}\varepsilon$ are the deviatoric components of the strain tensor ε_{ij}; $\varepsilon = \frac{1}{3}\varepsilon_{kk}$ = volumetric strain; δ_{ij} = Kronecker delta; $s_{ij} = \sigma_{ij} - \delta_{ij}\sigma$ = deviatoric stress components of stress tensor σ_{ij}; $\sigma = \frac{1}{3}\sigma_{kk}$ = volumetric stress. Subscripts i and j refer to Cartesian coordinates $x_i, i = 1,2,3$; K and G are the bulk and shear modulus; e''_{ij} = inelastic deviator strain; λ = inelastic dilatancy; Z_1 = constant; and ζ is a damage measure which is defined by

$$d\zeta = \frac{d\eta}{\left(1 + \dfrac{\beta_1\eta + \beta_2\eta^2}{1 + a_7 F_1}\right) F_2}; \qquad F_2 = 1 + \frac{a_8}{\left(1 + \dfrac{a_9}{\eta^2}\right) J_2(\underset{\sim}{\varepsilon})} \tag{10}$$

$$d\eta = \left\{ \frac{a_o}{1 - [a_6 I_3(\underset{\sim}{\sigma})]^{1/3}} + F_1 \right\} d\xi; \qquad d\xi = \frac{1}{2} de_{ij} de_{ij} \tag{11}$$

$$F_1 = \frac{a_2[1 + a_5 I_2(\underset{\sim}{\sigma})]\sqrt{J_2(\underset{\sim}{\varepsilon})}}{\{1 - a_1 I_1(\underset{\sim}{\sigma}) - [a_3 I_3(\underset{\sim}{\sigma})]^{1/3}\}[1 + a_4 I_2(\underset{\sim}{\sigma})\sqrt{J_2(\underset{\sim}{\varepsilon})}]} \tag{12}$$

The inelastic dilatancy variable λ is defined by

$$d\lambda = \frac{c_o}{1 - c_1 I_1(\underset{\sim}{\sigma})}\left(1 - \frac{\lambda}{\lambda_o}\right)\left\{\left(\frac{\lambda}{\lambda_o}\right)^2 + \left[\frac{J_2(\underset{\sim}{\varepsilon})}{c_2^2 + J_2(\underset{\sim}{\varepsilon})}\right]^3\right\} d\xi \tag{13}$$

and

$$K = \frac{E_o}{3(1 - 2\nu)}\left(1 - \frac{\lambda}{4\lambda_o}\right); \qquad G = \frac{E_o}{2(1 + \nu)}\left(1 - \frac{\lambda}{4\lambda_o}\right) \tag{14}$$

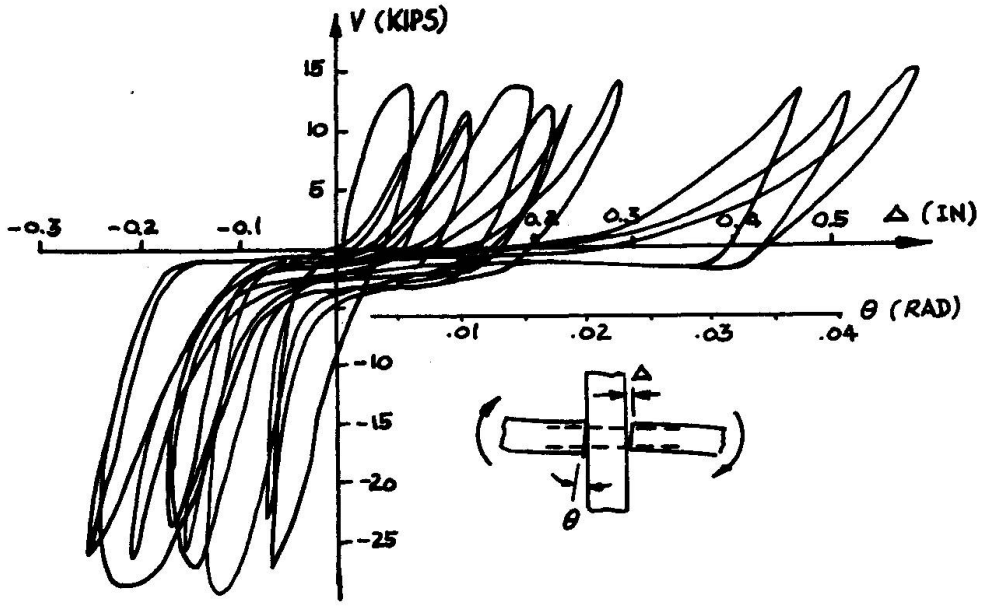

FIG. 3 SHEAR FORCE - BAR SLIP DIAGRAM (REF. 14)

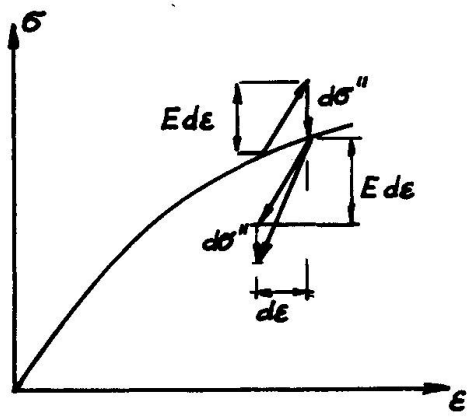

FIG. 4 STRESS-STRAIN LAW ENDOCHRONIC THEORY

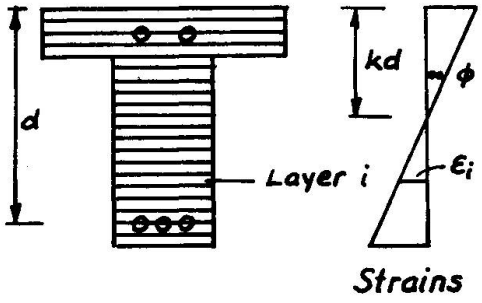

FIG. 5 ELEMENT LAYERS FOR T-SECTION

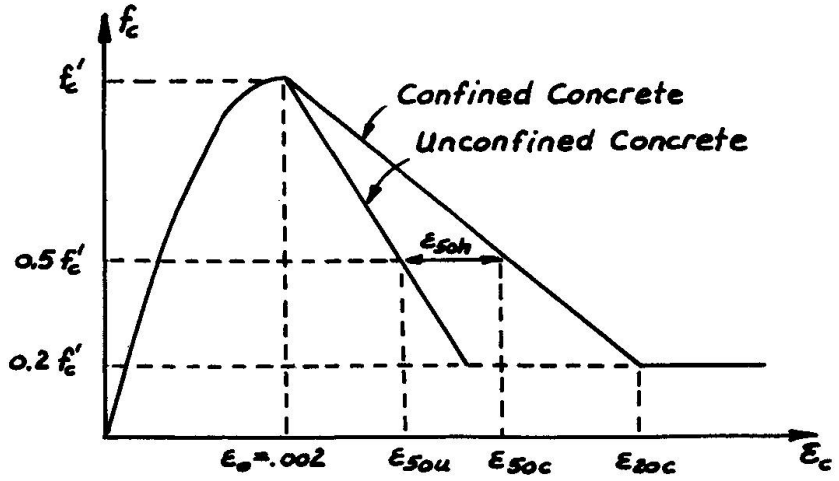

FIG. 6 CONCRETE STRESS-STRAIN LAW (REF. 25)

I_1, I_2, I_3 are the three invariants of the stress tensor, and J_2 is the second invariant of the deviator. The various material parameters can be determined by fitting the constitutive law to test data, such that normal-weight concretes are approximated remarkably well. The above formulation is fully continuous in that no inequalities are needed to distinguish between loading and unloading and various ranges of strain, Fig. 4. Bazant and Bhat claim that the endochronic theory is particularly effective in modeling cyclic responses, inelastic dilatancy due to large shear strains, strain-softening properties, and the hydrostatic pressure effect on triaxial behavior. The theory has been shown to match well the experimental uniaxial, biaxial, and triaxial stress-strain diagrams, including strain softening and failure envelopes, torsion-compression tests, lateral stresses, volume change, unloading and reloading diagrams, and cyclic loadings.

For numerical analysis it is more convenient to recast Eq. 9 in a matrix form, which reads

$$\underset{\sim}{\Delta\sigma} + \underset{\sim}{\Delta\sigma}'' = D\underset{\sim}{\Delta\varepsilon}$$

or

$$\begin{Bmatrix} \Delta\sigma_{11} + \Delta\sigma''_{11} \\ \Delta\sigma_{22} + \Delta\sigma''_{22} \\ \Delta\sigma_{33} + \Delta\sigma''_{33} \\ \Delta\sigma_{12} + \Delta\sigma''_{12} \\ \Delta\sigma_{23} + \Delta\sigma''_{23} \\ \Delta\sigma_{31} + \Delta\sigma''_{31} \end{Bmatrix} = \begin{bmatrix} D_{11} & D_{12} & D_{13} & 0 & 0 & 0 \\ & D_{22} & D_{23} & 0 & 0 & 0 \\ & & D_{33} & 0 & 0 & 0 \\ & (\text{symm}) & & D_{44} & 0 & 0 \\ & & & & D_{55} & 0 \\ & & & & & D_{66} \end{bmatrix} \begin{Bmatrix} \Delta\varepsilon_{11} \\ \Delta\varepsilon_{22} \\ \Delta\varepsilon_{33} \\ \Delta\varepsilon_{12} \\ \Delta\varepsilon_{23} \\ \Delta\varepsilon_{31} \end{Bmatrix} \qquad (15)$$

in which $\Delta\sigma''_{ij} = 2G\Delta e''_{ij} + 3K\Delta\lambda\delta_{ij}$; δ_{ij} is the Kronecker delta, and $D_{11} = D_{22} = D_{33} = K + 4G/3$; $D_{12} = D_{13} = D_{23} = K - 2G/3$; $D_{44} = D_{55} = D_{66} = 2G$.

Using this material model, the authors were able to correctly reproduce the response of reinforced concrete members under cyclic loading, without the need to adjust any values of the material parameters.

A number of authors have worked with elasto-plastic models which have the advantage of simplicity and computational efficiency [21,22,23]. However, they do not readily allow for effective incorporaton of stiffness degradation under load reversals and increased inelastic deformation and therefore may prove to be inadequate for a number of important applications.

5.2 Semi-Finite Element Models

Park, Kent and Sampson [24] have computed moment-curvature relationships for cyclic loading by subdividing the member section into a number of discrete layers, Fig. 5, with an assumed strain distribution as shown. Stresses in the concrete and steel of the various layers are determined directly from the assumed stress-strain law. With these stresses and the steel and concrete areas, the forces in each layer are easily computed. An iterative technique is then used to correct the assumed strain distribution, or more specifically, the neutral axis position, in order to satisfy the requirement that the sum of all forces acting on the section must be equal to the applied axial load.

The uniaxial stress-strain curve for concrete under monotonic load proposed by Kent and Park [25], Fig. 6, includes the effect of confinement which the authors claim has a major effect only on the unloading branch. The stress-strain curve for the steel reinforcement is modeled by using a Ramberg-Osgood formulation,

$$\varepsilon_s = \frac{f_s}{E_s}\left(1 + \left|\frac{f_s}{f_{ch}}\right|^{r-1}\right) \tag{16}$$

where f_{ch} and r are characteristic parameters chosen to fit experimental data. Using this formulation and a specific set of rules for unloading and reloading, the authors have achieved moderate success in reproducing moment-curvature as well as load-deflection diagrams of cyclically loaded beams and columns.

Ma, Bertero and Popov [26] have also adopted a Ramberg-Osgood formulation for the hysteresis model for reinforcing steel and have succeeded remarkably in reproducing cyclic test results. They also used the monotonic compressive stress-strain curve of Park and Kent as an envelope for cyclic concrete loading. Their improvements over the previous model lie primarily in the detailed rules for unloading and reloading, while the monotonic stress-strain curves for both steel and concrete are essentially the same. As a result, the agreement between theoretical and experimental moment-curvature diagrams is excellent.

Recently, Stanton and McNiven [27] have used system identification techniques to improve and extend Ma's work to include also a bond-slip model. With this work, semi-finite element models have reached a state of refinement where they offer promising potential for practical use.

5.3 Member-Size Models

Neither the finite element nor semi-finite element models are yet of much practical value because of the excessive effort needed to compute the moment-curvature relationship of a section. Realistic concrete structures consist of tens or hundreds of members for which stiffness properties have to be established and updated for each small time or load increment. In order to make a nonlinear analysis feasible, the model for concrete members will have to be simplified considerably. Thus, there is basically no choice but to rely on member-size models capable of describing the end force-end displacement or end moment-end rotation relationships with adequate accuracy, yet without a prohibitive amount of computational effort.

The first such model was the bilinear model proposed by Clough [28]. In its simple form this model cannot simulate the permanent stiffness degradation accompanying the progressive cracking of concrete during large inelastic excursions. In order to improve the model in this regard, Hidalgo and Clough [29] have introduced a stiffness degradation parameter with which the effective concrete modulus of elasticity is decreased uniformly throughout the structure. Since such a parameter has to be related to a maximum deformation response quantity, the maximum amplitude of the first generalized displacement or modal displacement was selected. Assuming that the modal matrix of the structure remains essentially unchanged even during large inelastic deformations, the nodal displacement vector $\{v\}$ can be transformed to modal or generalized coordinates,

$$\{Y\} = [\Phi]^T\{v\} \tag{17}$$

The value of Y_1 at which the first plastic hinge develops in the structure is defined to be the critical threshold beyond which the structure stiffness is effectively reduced.

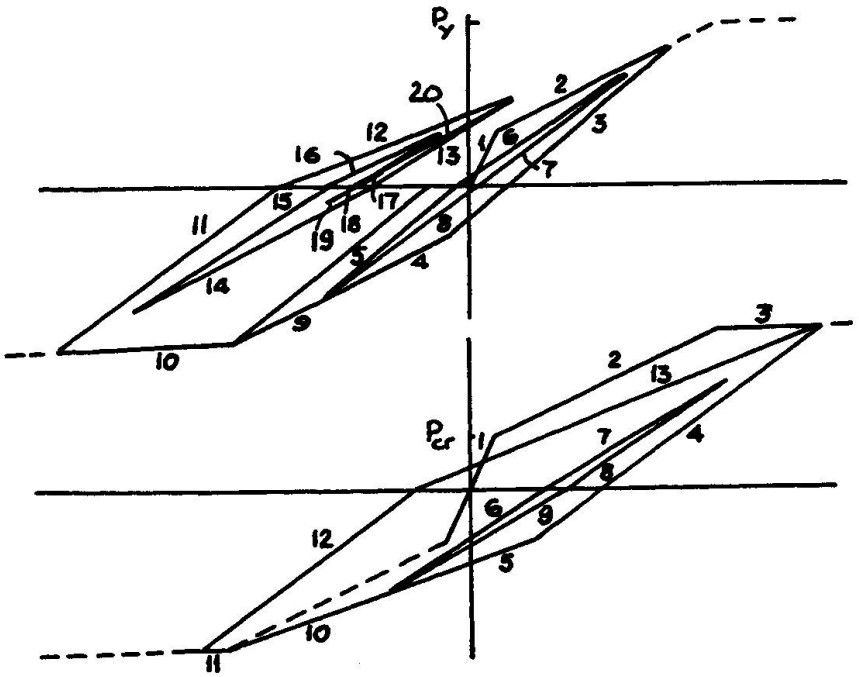

FIG. 7 EXAMPLES OF TAKEDA'S HYSTERESIS RULES (REF. 30)

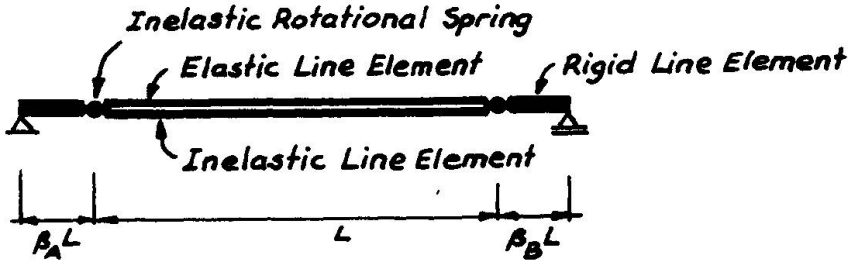

FIG. 8 OTANI'S MODEL (REF. 31)

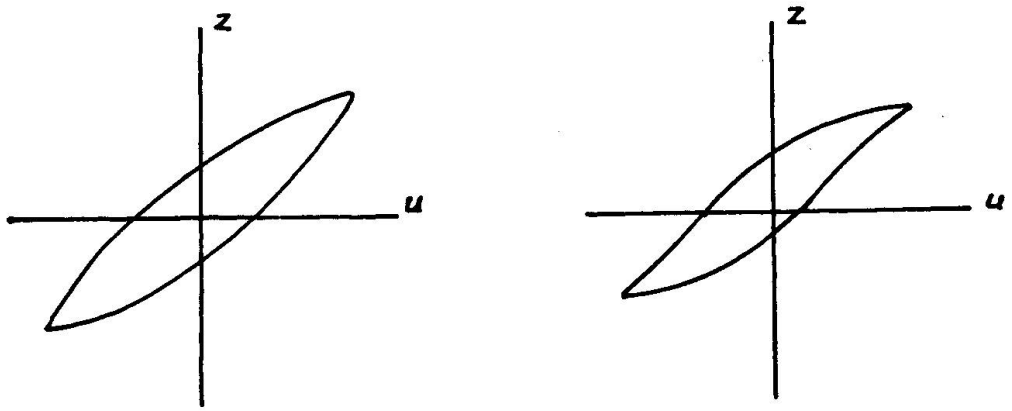

FIG. 9 EXAMPLES OF BABER AND WEN'S MODEL (REF. 32)

This study was rather specialized in that the model parameters were calibrated against test results for a simple two-story one-bay frame, but excellent agreement between experimental and analytical response histories was obtained. A trilinear model was proposed by Takeda, Sozen and Nielsen [30], Fig. 7, in conjunction with an elaborate set of hysteresis rules controlling the response under load reversals.

A somewhat different approach was followed by Otani [31] who added to the conventional bilinear or two-component model concentrated nonlinear springs, Fig. 8, in the vicinity of expected plastic hinges, i.e., near the clear span ends of a member. The flexibility constant of the spring can be adjusted to simulate bond deterioration of the reinforcing steel in the joint core as a function of the steel surface condition and stress history, and the degree of confinement and quality of the concrete. The idealized moment-curvature relationships for sections obtained from the assumed material laws led to results that compared reasonably well with test results for a three-story frame. However, the stiffness degradation mechanism, a simplified version of Takeda's model, tended to underestimate the response in the later phases of the time histories, during periods of reduced ground accelerations.

An interesting model was proposed recently by Baber and Wen [32], wherein four functions are combined to obtain a closed hysteresis loop with sufficient free parameters to model both softening and hardening materials, Fig. 9. The deterioration parameter was chosen to be a function of the total energy dissipated by hysteretic action, although according to some tests [10,13], rather stable hysteresis loops can be obtained, i.e., much energy dissipated without significant stiffness degradation. But the authors' primary objective was not so much to develop a model to accurately reproduce reinforced concrete behavior but rather to permit with relatively little expense the conduct of Monte Carlo type random vibration analyses.

The state of the art in modeling reinforced concrete behavior under cyclic loading has not yet progressed to the point where it is possible to reproduce experimental response data with a cost-effective member-size model that can account for both permanent stiffness degradation in flexural and shear behavior as well as bond deterioration in joint zones, However, it should be stressed that "perfect" match between analytical and experimental responses is neither possible nor particularly needed, because the dynamic response of concrete structures is associated with numerous uncertainties regarding the actual in-place material properties, geometric tolerances, and most significantly of all, the expected load history. The primary goal of mathematical modeling therefore consists rather of capturing the essential mechanical response characteristics within reasonable accuracy. Any remaining discrepancies are justifiably lumped together with the other probabilistic influence factors for assessing the safety or reliability of a complete reinforced concrete structure.

6. DYNAMIC ANALYSIS METHODS

In many situations it is difficult if not impossible to simulate the effects of dynamic loads acting on a structure by using equivalent static loads alone. In these cases, analysis methods have to be employed which take into account the important dynamic effects. These methods are based on the classical theory of vibrations and structural dynamics. For lumped parameter systems such as those resulting from a finite element discretization, the equations of motion can be written in matrix notation as

$$[M]\{\ddot{x}\} + [C]\{\dot{x}\} + [K]\{x\} = \{P(t)\} \qquad (18)$$

where $[M]\{\ddot{x}\}$ are the inertia forces and $[C]\{\dot{x}\}$ the viscous damping forces, proportional to velocity, but with constant damping matrix [C]. The dynamic or time-dependent forces $\{P(t)\}$ will in the most general case include the ground motion effect $-[M]\{\ddot{x}_g\}$. The static restoring forces $[K]\{x\}$ are normally nonlinear. This is particularly true for concrete structures for which the stiffness is not only amplitude- but also time-dependent, $[K] = [K(x,t)]$. The nonlinearity of Eq. 18 precludes the use of solution methods that are based on the principle of linear superposition such as the standard normal mode method. For this reason, direct integration methods are more appropriate. In particular, it is practical to solve the equations of motion in incremental steps of small time intervals Δt,

$$[M]\{\Delta\ddot{x}\} + [C]\{\Delta\dot{x}\} + [K]\{\Delta x\} = \{\Delta P(t)\} \tag{19}$$

The time step size Δt should be chosen small enough to allow an adequate definition of the forcing functions $\{P(t)\}$, which are normally assumed to vary linearly within a time step. The actual integration of Eqs.18 or 19 is performed by using one of the numerical integration algorithms that have been developed in recent years [33]. Unconditionally stable methods such as the Newmark β-method or Wilson θ-method deserve particular attention. These methods of integration readily permit constant updating of the structure stiffness $[K(x,t)]$ as prescribed by the mathematical model for the individual structural members. The formation and factorization of the structure stiffness which is normally very large for typical finite element analyses, requires a considerable amount of computational effort. Ways of reducing this effort are described in the literature [34,35].

In view of the randomness of many dynamic loads to which concrete structures may be subjected, it is helpful to divide analysis methods into two major categories, deterministic and probabilistic methods.

For deterministic methods of analysis, the forcing function P(t) is a precisely defined function which for numerical analysis purposes is normally specified in digitized or tabular form, i.e., sampled at a sufficient number of characteristic points to adequately represent the load. Examples for such deterministic loads are actually recorded time histories of earthquake ground accelerations or wind gusts or blast pressure impulse functions.

If the function P(t) is not given as an explicit time history, but only in terms of statistical parameters such as a power spectral density function and maximum intensity, then probabilistic methods of analysis will prove advantageous. For linear systems, the equations of motion are normally solved in the frequency domain. But if the equations are nonlinear because $[K] = [K(x,t)]$, then such methods become very difficult and are not appropriate for large finite element systems. In such cases it is preferable to use Monte Carlo techniques to artificially generate a number of random time histories with spectral properties and maximum intensity which are compatible with the statistical input requirements. The finite element model is then analyzed for each one of the artificial input forcing functions. In this fashion, an ensemble of sample response histories is generated which can be used as a basis for a statistical evaluation of expected maximum displacements, stress levels, cracking, etc. Such statistical information is of considerably more interest to the designing engineer than response values obtained from single deterministic analyses.

Impulsive loads such as blast and missile impact are so completely different from other loadings as to affect not only the modeling considerations but also the analysis methods. When analyzing missile impact problems by the finite element method, the constitutive laws should include the strain-rate dependency

of the material properties. The program should also allow for large displacements, slide lines and rezoning. A slide line permits relative slip to occur between finite elements representing the missile and the concrete target, or between portions of the target to allow modeling of a plug being pushed out ahead of the missile. Rezoning permits the division of the target into changing sets of elements during the course of the calculation. It is required in large deformation problems in Lagrangian formulation because the finite elements follow the material motion and may become excessively distorted. When rezoning occurs, the elements are laid out in a regular array, and the motions and stresses from the old elements are mapped into the new elements.

In certain problems involving missile impact or blast loadings, the dynamic response can be treated as wave propagation phenomenon. This can be analyzed by analytical methods only if the waves and structures can be sufficiently simplified, and the material properties assumed to be linear. Since these assumptions seldom apply to concrete structures, the use of discretiziation methods such as finite element or Lagrangian finite difference methods is necessary. Most large-capacity programs are restricted to continuum elements for which the nonlinear stress-strain properties of reinforced concrete are expressed in terms of continuum variables. Some authors have combined structural and continuum elements for those cases in which discrete structural elements such as beams, plates, or shells are embedded in soil or rock, which is treated as a continuum. Computer programs for such hybrid analyses have size limitations for the mathematical models.

Blast problems involving very high pressures can be addressed by treating the concrete as a fluid whose equations of state express the pressure as a function of relative density and specific internal energy.

7. CONCLUSIONS

Reinforced concrete exhibits an extremely complex behavior under dynamic loads, in particular if load reversals into the inelastic range are involved. This is true in the case of buildings subjected to such loadings as severe earthquake ground motions, missile impact or blast loadings. The advancement of numerical modelling techniques, in particular of finite element technology, has permitted researchers to simulate test results remarkably well, as long as shear degradation and bond deterioration do not play a major part in the response. For most practical purposes, however, these elaborate numerical techniques have primarily only academic value. What is needed are member-size models that not only capture the flexural response of reinforced concrete members adequately, but also include the shear degradation and bond deterioration, and which are simple enough to make the nonlinear analysis of realistic structures feasible.

8. ACKNOWLEDGEMENTS

Parts of this report are based on a state-of-the-art review currently being written for the ASCE Committee on Finite Element Analysis of Reinforced Concrete Structures. The contributions of Dr. A. A. Mufti of Nova Scotia Technical College to the review of finite element models and the help of Dr. J. Isenberg on blast load effects are acknowledged. Information on missile impact was provided by L. Seaman and Y. M. Gupta of SRI International.

REFERENCES

1. NEWMARK, N.M. and ROSENBLUETH, E., "Fundamentals of Earthquake Engineering," Prentice-Hall, Inc., Englewood Cliffs, 1971.
2. SIMIU, E. and SCANLAN, R.H., "Wind Effects on Structures," John Wiley and Sons, New York, 1978.
3. NEWMARK, N.M. and HALTIWANGER, J.D., "Principles and Practices for Design of Hardened Structures," Technical Documentary Report No. AFSWC-TDR-62-138, Air Force Special Weapons Center, 1962.
4. BERTERO, V.V., "Experimental Studies Concerning Reinforced, Prestressed and Partially Prestressed Concrete Structures and Their Elements," Symposium on Resistance and Ultimate Deformability of Structures Acted on by Well Defined Repeated Loads, IABSE, Lisbon, 1973.
5. TAYLOR, M., "Constitutive Relations for Concrete Under Seismic Conditions," Proceedings of Workshop on Earthquake-Resistant Reinforced Concrete Building Construction, Berkeley, Ca., July 1977.
6. MAHIN, S.A. and BERTERO, V.V., "Rate of Loading Effects on Uncracked and Repaired Reinforced Concrete Members," Earthquake Engineering Research Center Report No. EERC 72-9, University of Califronia, Berkeley, 1972.
7. OTANI, S., "Nonlinear Dynamic Analysis of Plane Reinforced Concrete Building Structure," Canadian Conference on Earthquake Engineering, McGill University, 1979.
8. SHIGA, T., OGAWA, J., SHIBATA, A. and SHIBUYA, J., "The Dynamic Properties of Reinforced Concrete Frames," Proceedings of the U.S.-Japan Seminar on Earthquake Engineering with Emphasis on the Safety of School Buildings, Sendai, 1970.
9. BERTERO, V.V., BRESLER, B. and LIAO, H., "Stiffness Degradation of Reinforced Concrete Members Subjected to Cyclic Flexural Loads," Earthquake Engineering Research Center Report No. EERC 69-12, University of California, Berkeley, 1969.
10. CELEBI, M. and PENZIEN, J., "Experimental Investigation into the Seismic Behavior of Critical Regions of Reinforced Concrete Components as Influenced by Moment and Shear," Earthquake Engineering Research Center Report No. EERC 73-4, University of California, Berkeley, 1973.
11. "Building Code Requirements for Reinforced Concrete," American Concrete Institute Standard 318-77, Detroit, Michigan, 1977.
12. PARK, R. and PAULAY, T., "Reinforced Concrete Structures," John Wiley and Sons, New York, 1975.
13. BERTERO, V.V., POPOV, E.P. and WANG, T.Y., "Hysteretic Behavior of Reinforced Concrete Flexural Members with Special Web Reinforcement," Earthquake Engineering Research Center Report No. EERC 74-9, University of California, Berkeley, 1974.
14. BERTERO, V.V. and POPOV, E.P., "Hysteretic Behavior of Ductile Moment-Resisting Reinforced Concrete Frame Components," Earthquake Engineering Research Center Report No. EERC 75-16, University of California, Berkeley, 1975.
15. SCHNOBRICH, W.C., "Behavior of Reinforced Concrete Predicted by Finite Element Method," Proceedings of the Second National Symposium on Computerized Structural Analysis and Design, George Washington University, Washington, D.C., 1976.
16. SCORDELIS, A.C., "Finite Element Modeling of Reinforced Concrete Structures," Proceedings of Special Seminar on Analysis of Reinforced Concrete Structures by Means of the Finite Element Method, Politecnico di Milano, 1978.
17. DARWIN, D. and PECKNOLD, D.A., "Inelastic Model for Cyclic Biaxial Loading of Reinforced Concrete," Civil Engineering Studies, SRS No. 409, University of Illinois, Urbana-Champaign, Illinois, 1974.

18. DARWIN, D. and PECKNOLD, D.A., "Nonlinear Biaxial Stress-Strain Law for Concrete," Journal of the Engineering Mechanics Division, ASCE, Vol. 103, No. EM4, April 1977.
19. BAZANT, Z.P. and BHAT, P.D., "Endochronic Theory of Inelasticity and Failure of Concrete," Journal of the Engineering Mechanics Division, ASCE, Vol. 102, No. EM4, August 1976.
20. BAZANT, Z.P. and BHAT, P.D., "Prediction of Hysteresis of Reinforced Concrete Members," Journal of the Structural Division, ASCE, Vol. 103, No. ST1, January 1977.
21. CERVENKA, V. and GERSTLE, K.H., "Inelastic Finite Element Analysis of Reinforced Concrete Panels Under In-Plane Loads," Civil Engineering Report, University of Colorado, Boulder, 1970.
22. YUZUGULLU, O. and SCHNOBRICH. W.C., "A Numerical Procedure for the Determination of the Behavior of a Shear Wall Frame System," ACI Journal, July 1973.
23. AGRAWAL, A.B., JAEGER, L.G. and MUFTI, A.A., "Crack Propagation and Plasticity of Reinforced Concrete Shear-Wall Under Monotonic and Cyclic Loading," Conference on Finite Element Methods in Engineering, Adelaide, Australia, 1976.
24. PARK, R., KENT, D.C. and SAMPSON, R.A., "Reinforced Concrete Members With Cyclic Loading," Journal of the Structural Division, ASCE, Vol. 98, No. ST7, July 1972.
25. KENT, D.C. and PARK, R., "Flexural Members with Confined Concrete," Journal of the Structural Division, ASCE, Vol. 97, No. ST7, July 1971.
26. MA, S.-Y.M., BERTERO, V.V. and POPOV, E.P., "Experimental and Analytical Studies on the Hysteretic Behavior of Reinforced Concrete Rectangular and T-Beams," Earthquake Engineering Research Center Report No. EERC 76-2, University of California, Berkeley, 1976.
27. STANTON, J.F. and McNIVEN, H.D., "The Development of a Mathematical Model to Predict the Flexural Response of Reinforced Concrete Beams to Cyclic Loads, Using System Identification," Earthquake Engineering Research Center Report No. EERC 79-02, University of California, Berkeley, 1979.
28. CLOUGH, R.W., "Effect of Stiffness Degradation on Earthquake Ductility Requirements," Structural Engineering Laboratory, Report No. 66-16, University of California, Berkeley, 1966.
29. HIDALGO, P. and CLOUGH, R.W., "Earthquake Simulator Study of a Reinforced Concrete Frame," Earthquake Engineering Research Center Report No. EERC 74-13, University of California, Berkeley, 1974.
30. TAKEDA, T., SOZEN, M.A. and NIELSEN, N.N., "Reinforced Concrete Response to Simulated Earthquakes," Journal of the Structural Division, ASCE, Vol. 96, No. ST12, December 1970.
31. OTANI, S., "Inelastic Analysis of R/C Frame Structures," Journal of the Structural Division, ASCE, Vol. 100, No. ST7, July 1974.
32. BABER, T.T. and WEN, Y.K., "Stochastic Equivalent Linearization for Hysteretic, Degrading Multistory Structures," Civil Engineering Studies, SRS No. 471, University of Illinois, Urbana-Champaign, Illinois, 1979.
33. BATHE, K.-J. and WILSON, E.L., "Numerical Methods in Finite Element Analysis," Prentice-Hall, Inc., Englewood Cliffs, 1976.
34. MEYER, C., "Inelastic Dynamic Analysis of Tall Buildings," Earthquake Engineering and Structural Dynamics, Vol. 2, 1974, pp. 325-342.
35. ALIZADEH, A. and WILL, G.T., "A Substructured Frontal Solver and Its Application to Localized Material Nonlinearity," Computers and Structures, Vol. 10, 1979, pp. 225-231.

Finite Element Modelling of Reinforced Concrete Structures

Eléments finis pour le calcul de structures en béton armé

Finite Elemente zur Berechnung von Stahlbetontragwerken

J.H. ARGYRIS
Professor of Aeronautics

G. FAUST
Research Associate

K.J. WILLAM
Privatdozent

Institute of Statics and Dynamics for Aerospace Systems, University of Stuttgart
Stuttgart, Fed. Rep. of Germany

SUMMARY

The state of the art in finite element modelling of reinforced concrete structures is examined in three areas

- the spatial idealisation of composite structures,
- the constitutive models for the short-term behaviour of concrete under triaxial conditions, and
- the computational implications of rate type-constitutive formulations on the structural level

RESUME

L'application de la méthode des éléments finis aux structures en béton armé est considérée sous trois aspects

- l'idéalisation spatiale des structures composites,
- les lois constitutives des matériaux pour le comportement tridimensionnel,
- les questions de calculs des structures pour un comportement inélastique des matériaux

ZUSAMMENFASSUNG

Der Beitrag beschäftigt sich mit der Finiten Element Methode und ihrer Anwendung im Stahlbetonbau. Drei Themen werden untersucht,

- die räumliche Idealisierung des Verbundwerkstoffes,
- die Formulierung von Stoffgesetzen für das Kurzzeitverhalten im dreiaxialen Bereich, und
- die rechentechnischen Fragen bei der Behandlung von inelastischen Werkstoffvorgängen auf der Tragwerksebene

1. INTRODUCTION

Modern computational techniques and, in particular, the finite element method have been used in nonlinear analysis of reinforced concrete structures for more than a decade [1], [2], [3], [4]. In spite of intensive research activities on the refinement of reinforced concrete models there are still several open questions, partly also because they have never been posed before the advent of computers in structural mechanics. Another source of discomfort are the difficulties in the prediction of the ultimate load behaviour of such simple structures as deep and over-reinforced beams. In contradistinction to simple limit analysis concepts of beams we recognise that two- and three-dimensional finite element idealisations trace the entire history of structural degradation starting from tensile cracking to the nonlinear deformation behaviour in compression up to crushing and debonding and other interactive effects between concrete and reinforcement. Therefore, the finite element model is today primarily a tool for interpreting experimental observations and for studying constitutive assumptions and their effects on the overall performance of the structure rather than a new method for standard design problems. Clearly, nonlinear solutions are very costly, especially if two- or three-dimensional idealisations are used and, in particular, if the limit load behaviour is of primary concern. In this case the integrity or rather the stability of the structure has to be assessed at increasing load levels whereby the overall nonlinear response behaviour is approximated by a series of linearised steps.

The long-term serviceability is normally assessed in the linear regime. Implicitly it is assumed that the dead and life loads are sufficiently small so that the nonlinearity in the elastic and inelastic deformations can be neglected. This is necessary for long-term creep predictions with the effective modulus methods, however, it is no prerequisite for step-by-step time marching strategies in which cracking and other nonlinear concrete effects are traced with the appropriate time-operators. This approach lends itself also to the finite element solution of environmental transients which can be readily combined with the time dependent inelastic analysis of structures. In this case the partitioned solution scheme leads to a staggered computational path in which the thermal and hygral effects are normally introduced into the equation of motion in the form of thermal expansion and shrinkage (one-way thermomechanical and hygrothermal coupling).

At this stage it might be worthwhile to reflect upon the underlying postulates for the finite element modelling of reinforced concrete structures. Clearly, the combined effect of spatial idealisation, constitutive assumption and computational path is critical for the predictive value of the final solution. In the following, these three aspects will be discussed and assessed in the light of recent finite element developments. The lack of agreement among leading researchers in this context is an indication that there is still a need for a better understanding of the mechanics of reinforced concrete structures and its characterisation in a computer-oriented solution environment. Certainly, there is some justification for self-criticism of the complexity and cost of extensive finite element studies, however, this computer-oriented method gives us a chance to project constitutive observations onto the structural level and to examine their effects on the overall response of the structure.

2. STRUCTURAL IDEALISATION

The finite element method is most successful when we are dealing with composite structures. The heterogeneity can be readily modelled with separate elements including special elements for the interface conditions.

The spatial idealisation of reinforced concrete structures requires homogenisation at various levels:

(i) the configuration of the composite and

(ii) the fracture response at localised failure.

In the following, these two aspects are briefly examined together with a discussion of modelling aspects of reinforced concrete frames, plates and shells.

2.1 Modelling of the composite material

On the microscale the heterogeneous composition of concrete, the cement stone, aggregate and adhesive bending is modelled with the same ease as the composite action of concrete, steel reinforcement and their various interaction mechanisms on the macroscale. On an even larger scale, the composite may be homogenised entirely and described by equivalent isotropic or anisotropic material properties. This latter approach is certainly suitable for fibre-reinforced concrete, however, for the usual reinforced concrete structures this averaging technique is only appropriate if the global behaviour of the structure is of interest in the working stress regime. Clearly, tensile cracking and other specific concrete phenomena can be considered in this case only by the corresponding degradation of the "equivalent" material properties. This indicates the basic shortcoming of homogenisation which can only account for the combined response behaviour in the form of an average.

In reinforced concrete the large difference of concrete and steel behaviour is normally accounted for by a discrete approach where the configuration and mechanical behaviour of each constituent is modelled individually by appropriate finite elements. Perfect bond is usually assumed in order to reduce the number of degrees of freedom and to avoid the inherent difficulties in assigning appropriate bond properties. In this way, the complex interaction problem is circumvented, however pull-out effects as well as tension stiffening, dowel action and spalling cannot be accounted for directly except by "corresponding" modifications of the stiffness and strength properties of the constituents.

2.2 Modelling of the fracture process

Another major problem arises at the ultimate load analysis of reinforced concrete components. Here progressive cracking and gradual damage accumulation leads eventually to the localisation of discrete failure zones. The numerical modelling of the entire response spectrum is one of the open problems in the finite element analysis of reinforced concrete components. There are basically two approaches for the spatial idealisation of cracking, damage and localised fracture, the

- smeared crack model, and the
- discrete crack model.

Computationally the smearing approach is far more convenient since the topology of the idealised structure remains intact and all local discontinuities due to cracking, fracture and localised damage are distributed evenly over the element domain. This averaging procedure fits the scope of continuum mechanics or rather strength of material and the nature of the finite element displacement method where continuity of the displacement field and boundedness of the stress field are inherent properties.

In contrast, the discrete crack approach poses complex computational problems since the topology and the finite element mesh changes with the history of crack propagation. Traditionally, the question of fracture initiation and fracture propagation is here dealt with within strength of material concepts in which e.g. tensile cracking is defined in terms of maximum stress or strain. In this case, the entire fracture model depends primarily on the spatial idealisation and thus fracture is a question of mesh refinement rather than one of an objective measure of stress intensity or damage per unit volume. Therefore, recent attempts are directed towards the development of fracture mechanics concepts for the failure prediction of concrete. The main difficulty is here that linear fracture mechanics provides only a statement of stability or rather catastrophic failure of a given crack, while slow crack propagation necessitates additional concepts such as blunting, localized plastification at the crack tip and also large deformations. Here the J -integral and alternative energy criteria are rather promising candidates since they are combined measures of stress and strain. It is intriguing that such models also account for gradient effects as long as they are referred to a unit volume which has e.g. the size of the aggregate. These latter concept requires however further studies and is the subject of current research activities.

2.3 Modelling of flexural components

A particularly difficult modelling task is the finite element idealisation of flexural components where the dimensionality of the structural configuration is normally reduced by one with the aid of the Kirchhoff hypothesis. The development of consistent beam, plate and shell elements is however by no means trivial even for the simple case of linear elastic behaviour and a homogeneous cross-section. The Kirchhoff kinematics complicates unduly the construction of sound displacement models which maintain the convergence requirements as well as full compatibility before and after deformation. This is particularly true for curved shell elements but also for flat elements where the different order of expansion for membrane and bending action is often a source of serious discomfort. Alternatively, these kinematic difficulties are avoided by mixed and hybrid models or so-called degenerate solid elements which do not enforce the Kirchhoff kinematics and allow for shear deformations. These so-called degenerate solid elements lead to an excessive number of degrees of freedom if cubic expansions are used. Therefore, selective integration is used in order to capture the bending behaviour with a lower expansion and a smaller number of degrees of freedom. This corresponds to a decomposition of the strain energy into different components and a balancing of membrane, bending and transverse shear contributions by reduced integration.

For nonlinear and inelastic material behaviour the situation becomes even more complex. In this case the integration over the thickness has to be carried out by numerical integration which corresponds in the case of piecewise constant approximations to the familiar layering of the cross-section. Clearly, the data volume and the computational effort for evaluating the element properties increases proportionally with the number of layers but the total number of structural degrees of freedom remains constant. There are various proposals to by-pass the layered idealisation of bending problems e.g. by using stress resultants (first and higher order moments) and the corresponding integral formulation of the material law. All these homogenisations through the thickness suffer from severe shortcoming of a continuous stress distribution over the thickness which excludes non-monotonic and non-proportional loading paths in elasto-plasticity (restriction to the deformation theory of plasticity). Moreover, the interaction of inelastic membrane and bending behaviour can be properly incorporated only for cases when the two sets of principal axes coincide while transverse shear effects are neglected altogether. This transverse shear is also problematic in the layered approach because it exceeds the plane stress formulation adopted in the Kirchhoff models. The degenerate

solid elements offer some resolution since they can resort to a full three-dimensional material law. On the other hand the selective integration introduces here another complication since the individual contributions to the strain energy are evaluated at different pivot points.

In summary, the modelling of frame, plate and shell elements is rather complex due to the peculiar behaviour of reinforced concrete. The layered approach is however sufficiently general although debonding and shear failure have to be excluded if we adhere to the Kirchhoff kinematics. For this reason the notion of a pure displacement model is normally given up and equilibrium considerations are invoked in order to incorporate transverse shear effects in a global fashion and to account for tension stiffening because of finite crackspacing.

3. CONSTITUTIVE MODELS

The finite element analysis of reinforced concrete structures is restricted primarily by the shortcomings of the underlying constitutive models. Although the spatial idealisation can be refined to capture every detail of the structural configuration within the scope of sophisticated two- and three-dimensional finite element packages, the material characterisation of the concrete and the interface conditions is rather limited. As a matter of fact, rather simple constitutive postulates are normally adopted for the strength and the deformation behaviour under biaxial and triaxial conditions. For ultimate load studies these assumptions must cover the entire loading regime because the post-failure range is often crucial for the overall reserve strength and the redistribution capacity of indeterminate structures. This stress transfer introduces locally non-proportional loading paths with extensive unloading regimes although the external loading is still increasing monotonically. The material degradation due to progressive damage leads finally to localised fracture in which high gradients mobilise additional strength reserves beyond the data which are normally obtained from uniform stress specimens. The influence of different loading rates is usually neglected for short-term loadings, however in dynamic environments and quasistatic creep problems it dominates the response behaviour and must be included. The ultimate failure behaviour of reinforced concrete composites depends to a large extent on the interface properties between concrete and steel. Clearly, under extreme loading conditions these effects become very important and affect the overall performance of the composite structure.

In the following, two aspects of the mechanical behaviour are considered, the strength and the deformation characteristics of concrete when subjected to uniaxial and multiaxial loadings. Historically, the bulk of experimental work was and still is directed towards the response in uniaxial compression, while the other facets of the mechanical behaviour are expressed in terms of this fundamental property. Because of the experimental difficulties, multiaxial testing was primarily concerned with the evaluation of the strength properties. Only recently have deformation data become available for test set-ups which are truly triaxial [5]. Therefore, the failure models are in general more advanced than the corresponding nonlinear deformation models in the pre- and post-failure regime. In some cases strength and deformation behaviour are considered to be entirely independent properties while other models such as hypoelastic and endochronic formulations contain no explicit strength statements whatsoever. At this stage it is worthwhile to scrutinise some established constitutive concepts for the multiaxial behaviour of concrete under short-term loading in the light of the recent results from the international testing program [5].

3.1 Strength models

We consider here the general case of triaxial concrete strength which should cover also the biaxial and uniaxial cases. The numerous papers on the subject indicate however that the generalisation of the uniaxial strength values to triaxial conditions is by no means a trivial task.

There are two basic postulates which are normally adopted in order to simplify the construction of triaxial failure conditions

- isotropy, and
- convexity in principal stress space.

The first assumption is introduced because of the triple-symmetry in the triaxial stress space and the inherent simplification of the failure model. In reality, progressive damage leads certainly to oriented anisotropies near ultimate behaviour which require however the formulation of failure conditions in the six-dimensional stress space instead of the three-dimensional space of principal stresses. Because of the inherent complexity and the lack of experimental evidence it is reasonable to assume "isotropic" behaviour up to failure and even thereafter in the post-failure regime.

Clearly, the maximum shear strength increases with hydrostatic compression and exhibits a pronounced dependence on the third stress invariant (synonymous to the direction in the deviatoric plane). In summary, it is widely accepted that the failure condition is a function of all three stress invariants [6], [7] and that it is poorly reproduced by the axisymmetric Drucker-Prager cone or paraboloid formulated originally by Schleicher.

Convexity is an assumption which is supported by global stability arguments in plasticity. Clearly, there are some questions on the validity of this postulate for concrete, particularly if local material instabilities are considered in the post-failure regime. For the initial failure surface however convexity in the principal stress space is generally accepted even though it does not necessarily imply convexity in the six-dimensional stress space because of the non-quadratic form of the third invariant. It is intriguing that an alternative representation in the strain space may also introduce non-convex surfaces in spite of a convex strength model in stress space. In principle, a strain representation of failure has computational advantages if we think of finite element displacement models and material stability studies. However, the failure condition is in strain space certainly far more irregular than in stress space.

There are two basic groups of failure models depending on the smoothness of the failure surface. The first class with discontinuous vurvatures follows essentially the traditional Mohr-Coulomb criterion with tension cut-off [8], [9]. The second class rests on the concept of an extended Drucker-Prager model which includes the effect of the third stress invariant [10], [11]. From a numerical standpoint the discontinuities complicate the analysis since the failure surface has to be divided into subregions and due to difficulties of defininga unique stress transfer path at the corners. On the other hand, the discontinuous failure description furnishes additional information on the type of failure (tensile-cracking or shear sliding) and the direction of failure. In contrast the continuous descriptions can not provide statements of this sort if no additional concepts such as normality are invoked.

A recent comparison of the triaxial test data of the international program indicates that the continuously curved strength models with all three stress invariants yield a close overall approximation of the experimental results [12]. The Fig. 1 illustrates the construction of the

five parameter model by the authors [10] which is made up of an elliptic approximation of the deviatoric trace and a parabolic description in the Rendulic plane. Fig. 2 shows the triaxial strength data of the BAM [7] in comparison to the hydrostatic prediction of the five para meter model using the least square values of [12]. The corresponding deviatoric results are displayed in Fig. 3 for $\sigma_a = -1.25\, f_c$. Fig. 4 shows the trace in the biaxial plane $\sigma_3 = 0$ which is the most severe test of the triaxial failure model because of the large magnification of approximation errors due to the very acute angle of intersection. The plots indicate satisfactory agreement whereby the strength ratios $\alpha_2 = f_t / f_c$ and $\alpha_u = f_b / f_t$ are fixed from the biaxial concrete data. Thus the deviatoric radial vectors ρ_1 , ρ_t at a given section $\sigma_a = -\xi$ are the only free optimisation variables for fitting specific triaxial strength data.

The failure surface in stress space is certainly a first step towards defining the concrete behaviour under triaxial conditions. Clearly, we have to pose additional questions such as – what happens to the failure surface when the loading path reaches this strength constraint? In one limiting case of ideally plastic behaviour, the failure surface remains fixed in stress space while in the other limiting condition of ideally brittle behaviour it collapses suddenly to another configuration of residual strength. The actual post-failure behaviour in compression but also in tension lies certainly somewhere in between these two extremes (continuous softening in kinematically constrained specimens). On the other hand, the material already degrades progressively in compression before the limiting strength is reached. Therefore, if we consider hardening the failure model can be also utilised to define the nonlinearity in the pre-failure regime. This leads us to the general question of nonlinear deformation behaviour in the pre- and post-failure regime (hardening-softening models for triaxial conditions) and its representation for triaxial conditions.

3.2 Nonlinear deformation models

Two classes of constitutive models can be distinguished

(i) algebraic stress-strain laws based on a total (finite) formulation, and
(ii) differential stress-strain laws based on an incremental (infinitesimal) formulation.

The first class involves invariably nonlinear algebraic equations (secant laws) which arise e.g. in nonlinear elasticity (hyperelasticity) and the deformation theory of plasticity. The main advantages of this secant stiffness formulation are primarily numerical such as the full error control via unbalanced load iteration (no drift) and the unproblematic treatment of softening. The principal disadvantages are well-known, the total stress-strain laws restrict the range of application to primarily monotonic loading regimes. This limitation is rather severe since there are only very few actual problems without local unloading due to stress redistribution and with a frozen pattern of principal axes. In praxis, however, these effects are disregarded and many developments for the ultimate load analysis of statically undetermined problems resort to the total form of the stress-strain law because of its simplicity.

The differential rate models involve invariably tangential stress-strain laws which arise typically in hypoelasticity, plasticity, endochronic theory or alternative inelastic evolution laws. The main advantages of this tangential stiffness formulation are linearity (the tangential material law normally depends on the state variables – stress, strain etc. – but not on their differentials) and the broad range of application to non-monotonic, non-proportional loading regimes. In contrast to hypoelastic and endochronic models a proper loading condition is introduced in the flow theory of plasticity which separates elastic from inelastic behaviour. Therefore, nonlinearity and damage are mobilised only if a certain stress-threshold (the yield

condition) is exceeded while no damage can accumulate below that value. Furthermore, normality and convexity guarantee a stable material law in accordance with the dissipation inequality which is violated by variable moduli techniques in which a loading concept is introduced arbitrarily in order to distinguish loading and unloading branches [13]. It should be noted that a pure rate formulation does not result by mere differentiation of the secant moduli in the total formulation of the stress-strain law [14].

The principal disadvantages of the rate models are well-known, they are primarily numerical since they require step by step integration. The accumulation of the linearisation errors might lead to a considerable drift if truly finite increments are used for advancing the tangential approach and if a refined error control is lacking. Moreover, the tracing of softening branches is complicated by local singularities at the limiting points for which geometric stiffness effects might be important and should be included.

Broadly speaking there are three families of constitutive relationships according to the underlying theory of nonlinear elasticity, elasto-plasticity and endochronic or internal variable theory, respectively. In spite of a centennium of concrete technology there is still no single constitutive model which covers all facets of the mechanical behaviour of concrete. Therefore, we must be satisfied at this stage with phenomenological models which reproduce specific aspects of the response behaviour without violating fundamental principles of mechanics. Clearly, the modelling itself is an underdetermined problem because of the inherent nonlinearity and even more so because of the history dependence. This latter property alters the scope of the formulation from a relatively "simple" description of nonlinear equilibrium states (algebraic approach) to the far more demanding characterisation of an evolutionary process (differential approach).

(i) Nonlinear elasticity models

This family of constitutive models describes the nonlinear deformation behaviour irrespectively of path-dependence. Their application is primarily directed towards monotonic loading regimes where no distinction must be made between loading and unloading behaviour. A priori, there is no limitation as far as proportional loading is concerned as long as an objective formulation is used which assures invariance with regard to coordinate transformations. The orthotropic models [15], [16], [17], [18] however assign different material properties to each principal direction, which should therefore remain fixed during the entire loading history if not a co-rotational definition of stress rate is used such as the Jaumann stress rate.

The principal task of constructing a nonlinear deformation model for multiaxial conditions can be recognised best from the uniaxial compression behaviour shown in Fig. 5. The hardening branch is fully defined by the initial modulus of elasticity E_o and the maximum strength σ_c where the tangent modulus approaches zero, $E_T = 0$. The associated strain ε_c defines the ductility when the maximum stress is reached. This tells us immediately that for a three-dimensional extension of the uniaxial law there is additional information required on the triaxial failure strain beyond the strength values discussed before. An alternative formulation resorts to the secant modulus $E_s = \sigma_c/\varepsilon_c$ at triaxial failure which is however only another statement of the failure strain ε_c which is normally very strongly path-dependent. As a result, there is no simple approach for constructing a nonlinear deformation model which should start initially with the linear elastic properties and should then introduce progressive damaging up to singular behaviour of the tangential material law at the maximum strength value. If we proceed further into the softening regime, and this is of utmost importance for the evaluation of the reserve strength, we have to define an additional rupture strain ε_r and possibly also a reserve strength σ_r. For general triaxial conditions this property is very

difficult to define, thus ideal plasticity is often assumed up to a maximum rupture strain ε_r where full strength degradation takes place, $E_r = 0$.

There have been several proposals of the tangential material law; most noteworthy are the developments of a nonlinear secant formulation [19] for E_s and ν_s introducing a nonlinearity index as a scalar measure of "equivalent" triaxial stress. A very recent proposal [18] adopts the concept of the equivalent orthotropic strain in [17] in order to construct an incremental orthotropic material law with the aid of the five parameter strength model. The orthotropic properties are however somewhat in conflict with the usual definition of hypoelasticity which exhibits stress induced anisotropy [20] but not orthotropic tangent moduli with reference to principal directions limiting the range of application ot proportional loading if not a so-called objective stress rate is used.

In contradistinction to the engineering models above there are some developments which follow the classical concepts of hyper- and hypoelasticity. It is intriguing that there are no attempts to describe the nonlinear deformation behaviour of concrete in terms of a strain energy function $U = U(\boldsymbol{\varepsilon})$ where the total stress-strain law

$$\boldsymbol{\sigma} = \frac{\partial U}{\partial \boldsymbol{\varepsilon}} \tag{3.1}$$

corresponds to the secant relationship

$$\boldsymbol{\sigma} = \mathbf{E}_s \boldsymbol{\varepsilon} \qquad \text{with} \qquad \mathbf{E}_s = \frac{\partial U}{\partial \boldsymbol{\varepsilon}}\, \boldsymbol{\varepsilon}^{-1} \tag{3.2}$$

The associated rate law derives by differentiation of (3.1)

$$\dot{\boldsymbol{\sigma}} = \mathbf{E}_T \dot{\boldsymbol{\varepsilon}} \qquad \text{with} \qquad \mathbf{E}_T = \frac{\partial^2 U}{\partial \boldsymbol{\varepsilon}\, \partial \boldsymbol{\varepsilon}^t} \tag{3.3}$$

Clearly, a quadratic power expansion of $U(\boldsymbol{\varepsilon})$ corresponds to linear stress-strain behaviour with $\mathbf{E}_T = \text{const}$. Thus a fourth order strain energy function would be required in order to obtain a rate formulation (3.3) of grade two. For isotropic conditions the strain energy can be expressed in terms of the strain invariants $U(\boldsymbol{\varepsilon}) = U(J_1, J_2, J_3)$, however a fourth order expansion still involves 9 material constants whose identification poses certainly a formidable problem.

Traditionally, this task is simplified by decomposing the strain energy into hydrostatic and deviatoric components. As long as interaction effects remain negligible, which is certainly true for metals, the response due to hydrostatic stresses is purely hydrostatic and that due to deviatoric stresses purely deviatoric. Therefore, the strain energy decomposes into

$$U(\boldsymbol{\varepsilon}) = U_0(J_1) + U_d(J_2', J_3') \tag{3.4}$$

In [21] it was shown that the deviatoric component U_d cannot depend on the third invariant J_3' of deviatoric strains, thus $U_d = U_d(J_2')$. As a result, the modelling of nonlinear elastic deformation reduces to the evaluation of two single functions which describe the nonlinear volumetric and deviatoric behaviour

$$\sigma_0 = 3 K_s(J_1)\, \varepsilon_0 \tag{3.5}$$

and

$$\sigma_d = 2 G_s(J_2')\, e_d \tag{3.6}$$

In [22] the K and G -approach was expressed in terms of the octahedral stress and strain components and applied successfully to interprete biaxial and recently also triaxial concrete data [23]. It was however noted that under truly triaxial conditions there is noticeable coupling between the hydrostatic response and the deviatoric loading. Therefore, the decomposition of $U = U_0(J_1) + U_d(J_2')$ is debatable and some form of coupling has to be introduced, see e.g. [24].

It is intriguing that the incremental K-G formulation is made up of two components and cannot be simplified to an expression involving only the tangent moduli [14] since differentiation of (3.6) yields

$$d\sigma_d = 2\left(e_d \frac{dG_s}{dJ_2'} dJ_2' + G_s\, de_d\right) \tag{3.7}$$

where $\frac{dG_s}{dJ_2'} dJ_2' = \frac{3}{2} \frac{G_T - G_s}{J_2'} e_d^t de_d$ and $G_T = G_s + J_2' \frac{dG_s}{dJ_2'}$ (3.8)

The resulting tangential material law is therefore identical with the equivalent elastoplastic hardening von Mises formulation if $K_T = \text{const}$ and monotonic loading is considered only.

This leads us to the direct formulation of a differential material law within the theory of hypoelasticity where

$$\dot{\sigma} = E_T \dot{\varepsilon} \qquad E_T = E_T(\sigma, \varepsilon) \tag{3.9}$$

In the concrete literature the only attempt [20] develops an incremental constitutive law of grade one (linear in stress). Higher order expansions are forbidding because of the large number of material parameters although hypoelasticity is restricted a priori to isotropic conditions. In this context it is intriguing that the associated failure criterion can be identified with singularities of the tangential material law when $\det E_T = 0$.

(ii) Plasticity models

Since most of the early finite element work on physical nonlinearities was directed towards elastoplastic computations it was natural to adopt hardening plasticity formulations for the nonlinear deformation behaviour of concrete in compression.

In contrast to the hypoelastic rate formulation the flow theory of plasticity accounts for path-dependence via the loading criterion. The inherent postulate of linear elastic unloading is certainly a first improvement when compared with the purely elastic formulation, however the lack of an elastic hysteresis for repeated unloading-reloading conditions exhibits

also shortcomings when compared with the experimental evidence in [25](the endochronic and rate dependent viscoplastic formulations offer here some improvement).

In plasticity theory the difficulties with the identification of the tangent moduli in (3.9) are avoided altogether by resorting to the concept of a flow rule which controls the evolution of the inelastic deformation $\dot{\eta}$ in terms of the yield surface $f(\sigma, \alpha) = 0$

$$\dot{\eta} = \dot{\lambda} \frac{\partial f}{\partial \sigma} \qquad \text{with} \qquad \dot{\bar{\eta}} = \dot{\lambda} \frac{\partial f}{\partial \sigma}^t \frac{\partial f}{\partial \sigma} \tag{3.10}$$

α denote e.g. the current values of the five parameter yield surface in [10], [27]. The associated hardening rule determines the rate of change of the current yield surface and the normality condition $\partial f/\partial \sigma$ the direction of inelastic strain rate $\dot{\eta}$.

The first finite element applications to concrete in compression resorted to the well-established concepts of the Huber-Mises theory disregarding hardening due to volumetric compression. In this case a single hardening function suffices to describe the nonlinear deviatoric action in terms of the von Mises equivalent stress-strain diagram. This is equivalent to the tangential shear modulus of the nonlinear elastic K-G formulation above, where $K_T = \text{const}$.

In order to include hydrostatic effects, the Drucker-Prager extension of the von Mises model was adopted in [26] whereby two intersecting conical yield surfaces were necessary in order to obtain satisfactory agreement with the triaxial failure surface in tension and compression. There is no longer a unique hardening function which covers the entire loading regime. As a matter of fact, the same disturbing observation was made by the authors in [27] where the five parameter model was adopted to describe hardening by an affine expansion of all parameters and softening by a translatory shift along the hydrostatic axis. The range of motion is shaded in Fig. 6 while Fig. 7 illustrates the corresponding hardening in uniaxial and biaxial compression.

In a recent publication [28] a three-parameter elasto-plastic strainhardening theory was presented for biaxial conditions in which the equivalent plastic strain rate was decomposed into two tensile and one compressive plastic strain parameters. Extending this approach to triaxial conditions the current configuration of the five parameter model [10] is now defined by 5 independent hardening functions $\alpha_1 \dots \alpha_5$ in terms of the inelastic work $A_i = \int \sigma \dot{\eta}$ or the inelastic strain measure $\bar{\eta} = \int (\dot{\eta}^t \dot{\eta})^{1/2}$. To this end the increment of equivalent plastic strain $\dot{\bar{\eta}}$ is decomposed into the five plastic strains $\eta_1 \dots \eta_5$ by the mapping

$$\dot{\eta}_i = \beta_i \dot{\bar{\eta}} \qquad \text{with} \qquad \sum_i \beta_i = 1 \tag{3.11}$$

The decomposition factors β_i define the participation of each plastic strain η_i in the overall hardening-softening whereby the sum of increments equals the increment of equivalent plastic strain increment $\dot{\bar{\eta}}$. The individual hardening rules for each parameter α_i of the five parameter yield surface are now

α_1: $f_t = f_t^0 + g_1(\eta_1)$ - uniaxial tension

α_2: $f_c = f_c^0 + g_2(\eta_2)$ - uniaxial compression

α_3: $f_b = f_b^0 + g_3(\eta_3)$ - biaxial compression

α_4: $g_1 = g_1^0 + g_4(\eta_4)$ - tensile shear at $\sigma_4 = -\xi$

α_5: $g_2 = g_2^0 + g_5(\eta_5)$ - compressive shear at $\sigma_4 = -\xi$

The hardening functions $g_i(\eta_i)$ define the motion of the current yield surface in terms of the plastic strain values η_i and thus the equivalent plastic strain $\bar{\eta}$. For an assumed distribution of participation factors β_i the hardening functions $g_i(\eta_i)$ must be identified from triaxial test data. Clearly, this is not a trivial task, also because the resulting yield surface must satisfy certain convexity requirements. Certainly in the simplest case of an affine expansion of the yield surface the current strength parameters α_i must have the same mormalised value which would correspond to the isotropic hardening plot in Fig. 6.

The formation of the ensuing differential material law follows the usual concepts of hardening plasticity, see e.g. [27], whereby the evaluation of the consistency rule $\dot{f}_i = 0$ for determining $\dot{\bar{\eta}}$ involves now differentials with regard to the five strain hardening parameters $\alpha_1 \cdots \alpha_5$.

In completion we should note the intriguing development of endochronic time models which provide a very accurate description of the nonlinear concrete behaviour [29]. Since no proper justice can be done to this topic in this context we only recall that there is little difference between plasticity and endochronic theory when a loading condition is introduced [30] except for the formulation in total strain space and the intricate mappings relating total strain with endochronic time. Without the unloading condition the endochronic model predicts continuous damage accumulation even at very low stress levels which has been criticised particularly for dynamic applications [31]. An interesting alternative to the endochronic theory was presented recently in [32] where the incremental plasticity theory for hardening was combined with an elastic fracturing theory for softening, thus bypassing the difficulties with non-positive definite tangential material with the aid of a total secant formulation. Different aspects of all these constitutive models for concrete were examined recently in [33].

4. COMPUTATIONAL ASPECTS

On the structural level the total and differential forms of constitutive laws lead immediately to the well-known secant and tangential stiffness methods after appropriate discretisation with finite elements. The former approach determines directly the steady state equilibrium configuration by an iterative search technique while the latter traces the entire evolution path up to a certain state by tangential linearisation. The rate formulation involves thus the numerical integration of the entire process during which path-dependent effects are readily accounted for in contradistinction to the total equilibrium approach.

In the following, we examine different forms of incremental solution strategies for tracing the path of evolution of inelastic material processes. For illustration we will concentrate on elastic-viscoplastic material behaviour where the step by step integration is carried out in real time instead of a mechanically equivalent loading parameter which is used for rate-independent material problems.

The finite element method for elastic and inelastic material problems is well established. Therefore, we restrict ourselves to a brief summary of incremental equilibrium (principle of virtual power)

$$\int_V \delta \boldsymbol{\gamma}^t \Delta \boldsymbol{\sigma} \, dV = \int_V \delta \mathbf{u}^t \Delta \mathbf{p}_v \, dV + \int_S \delta \mathbf{u}^t \Delta \mathbf{p}_s \, dS \tag{4.1}$$

and the four classes of elastic-inelastic solution strategies which arise from different time integration methods of the constitutive rate equations [34], [35].

4.1 Initial load methods

First we recall the traditional initial load strategies where the time operator is partitioned into an elastic and inelastic component. The elastic stiffness is used here as reference stiffness which is maintained constant during the entire evolution of the viscoplastic rate process

$$\dot{\eta} = \mathbf{f}(\boldsymbol{\sigma}) = \frac{\mu}{\bar{\sigma}} \left(\frac{\bar{\sigma}}{\sigma_y} - 1 \right) \boldsymbol{\sigma}_d \tag{4.2}$$

In the case of the direct forward approach the inelastic growth law is approximated by the explicit statement

$$\Delta \boldsymbol{\eta} = \Delta t \, \dot{\boldsymbol{\eta}} = \Delta t \, \mathbf{f}_0 \tag{4.3}$$

where $\mathbf{f}_0$ indicates that only known state variables at the beginning of the time step are used $\mathbf{f}_0 = \mathbf{f}(\boldsymbol{\sigma}_0)$. The corresponding stress increment follows from the hypoelastic law

$$\Delta \boldsymbol{\sigma} = \mathbf{E} (\Delta \boldsymbol{\gamma} - \Delta t \, \mathbf{f}_0) \tag{4.4}$$

Substituting (4.4) into (4.1) yields the classical forward initial load method without iteration

$$\mathbf{K} \Delta \mathbf{r} = \Delta \mathbf{R} + \Delta \mathbf{J}_\eta^0 \qquad \text{with} \qquad \Delta \mathbf{r} = \mathbf{r}_1 - \mathbf{r}_0 \tag{4.5}$$

where $\mathbf{K}$ denotes the elastic stiffness matrix and $\Delta \mathbf{J}_\eta^0$ the initial loads due to the inelastic strain increment $\Delta \boldsymbol{\eta} = \Delta t \mathbf{f}_0$. The corresponding implicit formulation of the inelastic growth law involves yet unknown stresses within the time step Δt and thus requires iteration. The successive substitution method leads to a predictor-corrector scheme which updates the stress increment (4.4) according to the current values of the state variables, e.g. at the end of the time step if an overstable backward time operator is used

$$\Delta \boldsymbol{\sigma}^{i+1} = \mathbf{E} (\Delta \boldsymbol{\gamma}^i - \Delta t \mathbf{f}^i) \tag{4.6}$$

On the structural level we recover the iterative initial load method

$$\mathbf{K}\,\Delta\mathbf{r}^{i+1} = \Delta\mathbf{R} + \Delta\mathbf{J}_{\eta}^{i} \tag{4.7}$$

in which the inelastic strain increment is corrected iteratively according to the current stress values within the time step Δt .

4.2 Gradient methods

The application of the initial load methods is severely constrained by the time step restriction for stability and convergence [34], [35]. Although the resulting time marching strategy assures a very accurate viscoplastic solution it is rather expensive when the entire transient response history has to be integrated. The tangential stiffness methods are able to overrule these time step restrictions and thus provide more flexibility although at the cost of more elaborate computations.

In the case of the forward gradient approach the stress increment is defined by

$$\Delta\boldsymbol{\sigma} = \mathbf{E}_{T}^{o}\left(\Delta\boldsymbol{\gamma} - \Delta t\,\mathbf{f}_{o}\right) \qquad \text{where} \qquad \mathbf{E}_{T}^{o} = \left(\mathbf{E}^{-1} + \Delta t\,\frac{\partial \mathbf{f}_{o}}{\partial \boldsymbol{\sigma}}\right)^{-1} \tag{4.8}$$

In the forward strategy the tangential material law $\mathbf{E}_{T}^{o}$ and the inelastic growth law $\mathbf{f}_{o}$ are both evaluated at the beginning of the time step. Therefore no iteration is required and the computation on the structural level corresponds to the simplest form of the incremental tangential stiffness method without iterative correction

$$\mathbf{K}_{T}^{o}\,\Delta\mathbf{r} = \Delta\mathbf{R} + \Delta\mathbf{J}_{\eta}^{o} \tag{4.9}$$

In this method the time steps are limited by accuracy rather than stability. Moreover, the viscoplastic overstress model introduces elastic unloading effects when too large time steps are used. In this case, when the long-term steady state conditions are of prime concern, the backward gradient approach must be used in spite of the computational complexities with the resulting Newton-Raphson scheme.

In the Newton-Raphson technique the residual $\boldsymbol{\delta}^{i}$ of the incremental constitutive relations is reduced to zero

$$\boldsymbol{\delta}^{i} = \Delta\boldsymbol{\gamma}^{i} - \Delta t\,\mathbf{f}^{i} - \mathbf{E}^{-1}\Delta\boldsymbol{\sigma}^{i} \qquad \text{and} \qquad \boldsymbol{\delta}^{j+1} = \boldsymbol{\delta}^{j} + d\boldsymbol{\delta}^{j} = \mathbf{0} \tag{4.10}$$

The resulting stress corrections at the end of the time step are then

$$d\boldsymbol{\sigma}^{j} = \mathbf{E}_{T}^{j}\left(d\boldsymbol{\gamma}^{j} - \boldsymbol{\delta}^{j}\right) \tag{4.11}$$

where the tangential material law is evaluated at the end of the time step

$$\mathbf{E}_{T}^{i} = \left(\mathbf{E}^{-1} + \Delta t\,\frac{\partial \mathbf{f}^{i}}{\partial \boldsymbol{\sigma}}\right)^{-1} \tag{4.12}$$

On the structural level the unbalanced load due to the change of internal stresses $d\sigma^j$ is at the end of the time step

$$\int_V \delta\gamma^t \, d\sigma^j \, dV = R_1 - \int_V \delta\gamma^t \sigma_1^j \, dV \tag{4.13}$$

Substituting (4.11) into the incremental equilibrium condition (4.13) yields the tangential relation for the displacement correction dr

$$K_T^j \, dr^j = F^j \tag{4.14}$$

K_T^j denotes here the tangential structural stiffness corresponding to E_T^j in (4.12) and F^j the unbalanced load due to the constitutive error δ^j (4.10)

$$F^j = R_1 + \int_V \delta\gamma^t \left(E_T^j \left(-\Delta\gamma^j + \Delta t \, f^j + E^{-1} \Delta\sigma^j \right) - \sigma_1 \right) dV \tag{4.15}$$

As indicated before, the straight Newton-Raphson algorithm calls for formation and factorisation of the structural gradient matrix E_T^j at each cycle of iteration. The computational effort can be reduced by updating the tangential stiffness only occasionally, e.g. at the beginning of a new time step (modified Newton-Raphson technique). In the limit we maintain the elastic stiffness as structural gradient matrix during the entire viscoplastic process and recover the iterative initial load method above. However, the convergence limitations of this approach ask for alternative computational strategies such as the quasi-Newton methods. The most promising candidate is the BFGS-algorithm of Broyden-Fletcher-Goldfarb and Shanno which was developed originally in the context of optimisation and which was subsequently applied to different finite element problems [35], [36], [37].

4.3 BFGS-method

The quasi-Newton method is essentially a search technique for the new solution r_{k+1} according to

$$r_{k+1} = r_k + s_k \, d_k \tag{4.16}$$

using the secant relation

$$K_k \, \delta_k = \gamma_k \qquad \left\{ \begin{array}{ll} \text{where} & \delta_k = r_k - r_{k-1} \\ \text{and} & \gamma_k = F_k - F_{k-1} \end{array} \right. \tag{4.17}$$

The vector d_k denotes the search direction and s_k the scalar which satisfies the orthogonality condition

$$d_k^t \, F_{k+1} = 0 \tag{4.18}$$

The BFGS-method is based on a series of rank two modifications which can be directly applied in order to update the inverse K^{-1}

$$K_{\ell}^{-1} = \left(I + w_{\ell} v_{\ell}^{t}\right) K_{\ell-1}^{-1} \left(I + v_{\ell} w_{\ell}^{t}\right) \tag{4.19}$$

where the new search direction follows from

$$d_{\ell} = K_{\ell}^{-1} F_{\ell} \tag{4.20}$$

The scalar S_{ℓ} is obtained by line search for zero F_{ℓ} along d_{ℓ} if the orthogonality condition (4.18) exceeds an assumed threshold. The modification vectors v_{ℓ} and w_{ℓ} are defined as

$$v_{\ell} = F_{\ell-1}\left(1 + S_{\ell-1}\left(\frac{d_{\ell-1}^{t} \gamma_{\ell}}{d_{\ell}^{t} F_{\ell-1}}\right)^{1/2}\right) - F_{\ell} \tag{4.21}$$

$$w_{\ell} = \frac{1}{d_{\ell}^{t} \gamma_{\ell}} \delta_{\ell} \tag{4.22}$$

Note the index ℓ is used here in order to distinguish the BFGS-iteration from the Newton step (4.14) and the predictor-corrector method (4.7). Clearly, a sufficiently large number of BFGS-modifications correspond to a single Newton step, thus asymptotically we maintain the same range of convergence and circumvent the tight time step restrictions of the iterative initial load method. On the computational side the BFGS-method involves repeated modification of the triangular factor. The recursion formula (4.19) indicates that each iteration cycle involves a series of vector operations on the right-hand side. Clearly, for an efficient solution the number of iterations must be limited to a small number since the computational effort grows rapidly with each additional iteration. Normally, 3 - 7 iterations were sufficient to attain satisfactory convergence for large time step viscoplastic solutions where the elastic stiffness is retained as reference stiffness.

COMPUTATIONAL METHOD	DIRECT FORWARD $\zeta = 0$	ITERATIV CORRECTION $\zeta > 0$
INITIAL LOAD $E \longrightarrow K$	DIM $\Delta t < \Delta t_s$ $K \Delta \sigma = \Delta R + \Delta S_{\eta}^{0}$	NIM $\Delta t < \Delta t_c$ $K \Delta \sigma^{i} = \Delta R + \Delta S_{\eta}^{i}$
TANG. STIFFNESS $E_T \longrightarrow K_T$	DTS $K_T^{0} \Delta \sigma = \Delta R + \Delta S_{\eta}^{0}$	N-R $K_T^{i} d\sigma^{i} = F_{\zeta}^{i}$ BFGS: $\sigma_{k+1} = \sigma_k + s_k d_k$

Table 1: COMPUTATIONAL STRATEGIES FOR VISCOPLASTIC ANALYSIS

The four computational strategies are summarised in Table 1. The BFGS-method belongs to the class of iterative gradient methods, although the viscoplastic implementation operates with a constant elastic reference stiffness analogous to the iterative initial load method. The initial load methods exhibit stringent stability and convergence limits Δt_s, Δt_c which severely restrict the time steps [34]. It is intriguing that for rate independent plasticity no such convergence limit exists if the NIM-method is implemented within the initial stress formulation [38].

4.4 Viscoplastic solution of pressurised cylinder

For illustration we consider a thick-walled cylinder which is subjected to increasing internal pressure. Both the nonlinear response behaviour and the limit load behaviour are of interest when a viscoplastic overstress model is used to predict the transient phase up to steady state conditions. For simplicity a nonhardening viscoplastic model using (4.2) is used with $\sigma_y = const.$ in order to compare the steady state solution with that of the elastic - ideally plastic solution of Prager and Hodge [39].

Fig. 8 shows the basic lay-out and the idealisation with axisymmetric finite elements. The particular material properties are taken from a previous study [40] and are typical for a mild steel with

$$E = 30 \times 10^6 \text{ psi} \quad , \quad \nu = 0.30$$
$$\sigma_y = 30 \times 10^3 \text{ psi} \quad , \quad \mu = 10^{-8} \text{ sec/psi} \tag{4.23}$$

Fig. 9 shows the load-displacement relationship under increasing pressure. The solid line indicates the steady state elastic - ideally plastic solution which bounds the nonlinear response between the elastic limit $p_e = 12968$ psi and the plastic limit pressure $p_p = 24011$ psi . In the viscoplastic analysis various pressure levels ($p_i = 13$, 18, 21, 24 and 25×10^3 psi) were applied directly without incrementation, and the ensuing viscoplastic response was traced starting from the initial elastic overstress condition up to the steady state solution which approaches asymptotically the elastic-plastic response at $t \to \infty$. Even for an internal pressure of $p_i = 24000$ psi a stable steady state solution was reached while for $p_i = 25000$ psi the remaining overstress resulted in continuous outward flow.

The intrinsic performance of the previous computational strategies is illustrated with the equivalent stress history at the inside wall. Fig. 10 compares the prediction of the BFGS-algorithm with that of the direct forward methods with and without tangential stiffness. In the case of the DIM forward initial load scheme the constant time steps $\Delta t = 1$ sec lead to elastic unloading because of the critical time step for stability $\Delta t_s = 1.3$. In contrast the implicit BFGS algorithm provides high accuracy and exhibits far less numerical damping than the DTS forward gradient strategy. Note that the elastic stiffness matrix was retained in the BFGS and the DIM algorithms during the entire viscoplastic process while satisfactory convergence was obtained with the BFGS quasi-Newton method within 2 - 3 iterations.

Finally, the rapid deterioration of the forward gradient solution is shown in Fig. 11 where the equivalent stress distribution across the cylinder wall is plotted for a larger time step of $\Delta t = 10$. In this case , only the backward time operator is suitable for predicting the steady state condition within a single time step since the initial elastic overstresses relax to zero and lead to oscillations if they are included in the forward and midstep algorithms. As a

matter of fact, the forward gradient method utilises only the initial elastic information at the beginning of the time step for the evaluation of the tangential stiffness matrix. This aspect leads to forward gradient predictions which are completely erroneous for large time steps such as $\Delta t = 1000$, while the BFGS-algorithm yields still satisfactory results of the steady state elastic plastic solution within 13 iterations.

In conclusion, the BFGS-quasi-Newton method is very flexible - it provides very accurate solutions in the transient response regime and it readily accomodates very large time steps when the limiting steady state plastic solution is of primary concern. The viscoplastic solution is obtained with an elastic stiffness matrix which remains constant during the entire time history analysis. Therefore the BFGS-algorithm corresponds formally to the traditional initial load methods where the entire inelastic process is converted into equivalent driving forces on the right-hand side.

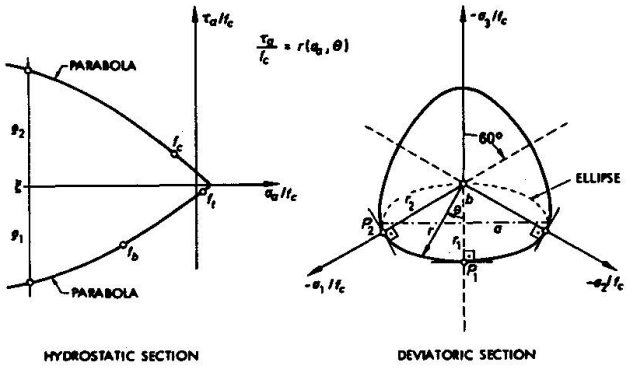

Fig. 1 CONSTRUCTION OF FIVE PARAMETER MODEL

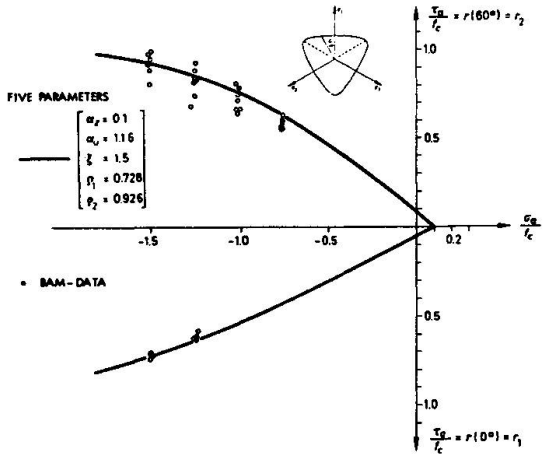

Fig. 2 FIVE PARAMETER MODEL, HYDROSTATIC SECTION

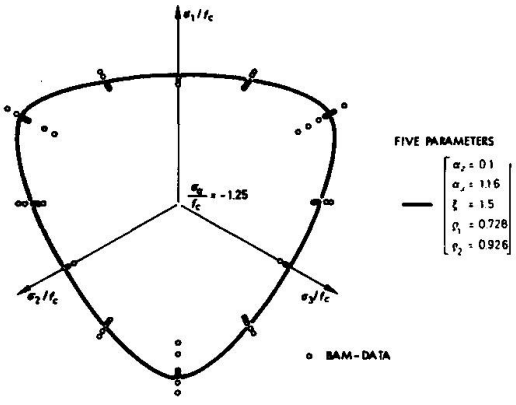

Fig. 3 FIVE PARAMETER MODEL, DEVIATORIC SECTION

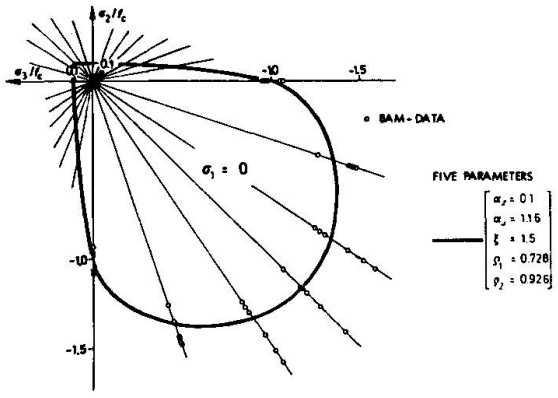

Fig. 4 FIVE PARAMETER MODEL, BIAXIAL SECTION

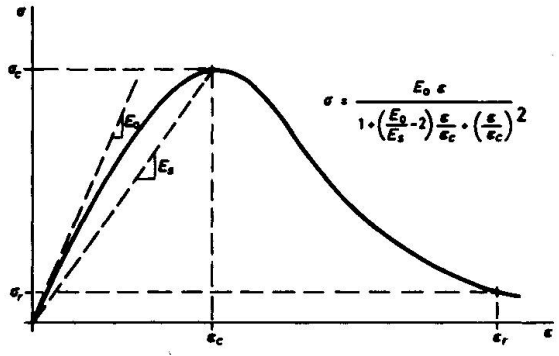

Fig. 5 UNIAXIAL COMPRESSION MODEL

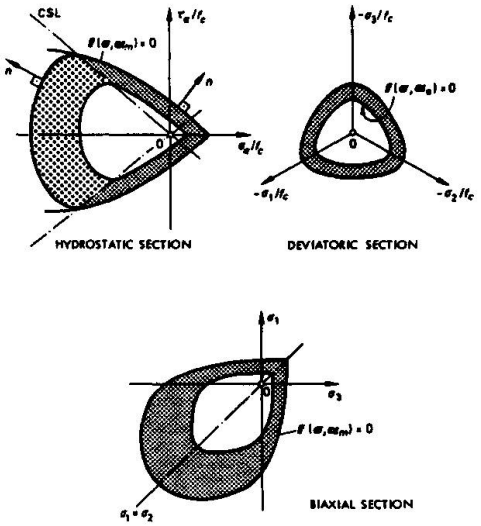

Fig. 6 HARDENING FIVE-PARAMETER MODEL

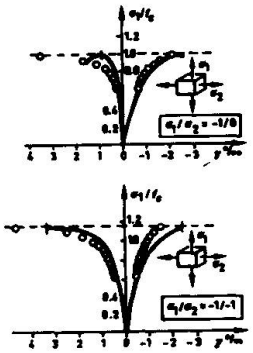

Fig. 7 COMPARISON WITH BIAXIAL TEST DATA [KUPFER et al]

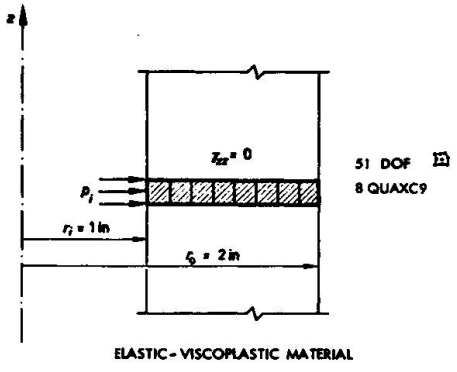

Fig. 8: THICK-WALLED CYLINDER UNDER INTERNAL PRESSURE

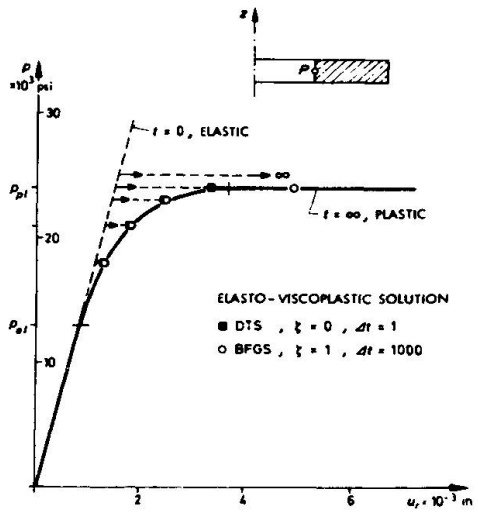

Fig. 9: LOAD-DISPLACEMENT BEHAVIOUR

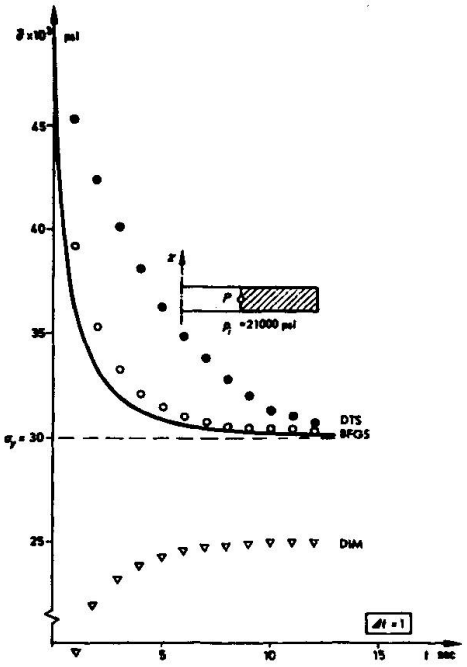

Fig.10: EQUIVALENT STRESS HISTORY AT THE INSIDE WALL

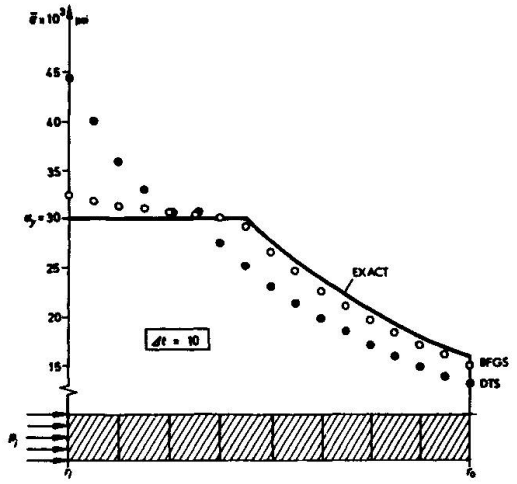

Fig.11: EQUIVALENT STRESS DISTRIBUTION AT THE TIME t = 10 sec

REFERENCES

[1] A.C. SCORDELIS, Finite Element Analysis of Reinforced Concrete Structures, The Finite Element Method in Civil Engng. (McGill Univ. Montreal 1972)

[2] J.H. ARGYRIS, G. FAUST, J. SZIMMAT, E.P. WARNKE, K.J. WILLAM, Recent Developments in the Finite Element Analysis of Prestressed Concrete Reactor Vessels, Nucl. Eng. Design. 28 (1974) 42-75

[3] W.C. SCHNOBRICH, Behaviour of Reinforced Concrete Structures Predicted by the Finite Element Method, Comp. Struct. 7 (1977) 365-376

[4] P.G. BERGAN, I. HOLLAND, Nonlinear Finite Element Analysis of Concrete Structures, Comp. Meths. Appl. Mech. Eng. 17/18 (1979) 443-467

[5] K.H. GERSTLE, D.H. LINSE et al., Strength of Concrete under Multiaxial Stress States, Proc. McHenry Symp., ACI SP55, Mexico City, 1976

[6] D.H. LINSE, H. ASCHL, Versuche zum Verhalten von Beton unter mehrachsiger Beanspruchung, Internal Report of Concrete Institute, Technical University Munich (1976)

[7] G. SCHICKERT, H. WINKLER, Versuchsergebnisse zur Festigkeit und Verformung von Beton bei mehraxialer Druckbeanspruchung, DAfStb Heft 277, 1977

[8] B. PAUL, Macroscopic Criteria for Plastic Flow and Brittle Fracture, in Fracture, an Advanced Treatise, H. Liebowitz ed., Academic Press (1968) 313-491

[9] J.H. ARGYRIS, G. FAUST, K.J. WILLAM, Limit Load Analysis of Thick-Walled Concrete Structures - A Finite Element Approach to Fracture, Comp. Meths. Appl. Mech. Eng. 8 (1976) 215-243

[10] K.J. WILLAM, E.P. WARNKE, Constitutive Model for the Triaxial Behaviour of Concrete, ISMES Seminar on Concrete Structures Subjected to Triaxial Stresses, Bergamo, May 17-19, 1974, Proc. IABSE Report No. 19, Zurich, 1975

[11] N.S. OTTOSEN, A Failure Criterion for Concrete, J. ASCE EM4 (1977) 527-535

[12] J. WASTIELS, Failure Criteria for Concrete under Multiaxial Stress States, Proc. IABSE Coll. on Plasticity in Reinforced Concrete, Copenhagen, May 21-23, 1979

[13] I. NELSON, M.L. BARON, I.S. SANDLER, Mathematical Models for Geological Materials for Wave Propagation Studies, Shock Waves and the Mechanical Properties of Solids, Syracuse University Press, Syracuse, N.Y. (1971)

[14] D.W. MURRAY, Octahedral Based Incremental Stiffness Matrices, ASCE, 105, EM4 (1979) 501-514

[15] T.C.Y. LIU, A.H. NILSON, F.O. SLATE, Biaxial Stress-Strain Relations for Concrete, ASCE 98, ST5 (1972) 1025-1034

[16] J. LINK, Eine Formulierung des zweiaxialen Verformungs- und Bruchverhaltens von Beton, Deutscher Ausschuß für Stahlbeton, Heft 270, Berlin 1976

[17] D. DARWIN, D.A. PECKNOLD, Nonlinear Biaxial Stress-Strain Law for Concrete, ASCE EM2 (1977) 229-241

[18] A.A. ELWI, D.W. MURRAY, A 3 D Hypoelastic Concrete Constitutive Relationship, ASCE 105, EM4 (1979) 623-641

[19] N.S. OTTOSEN, Constitutive Model for Short-Term Loading of Concrete, ASCE 105, EM1 (1979) 127-141

[20] M.D. COON, R.J. EVANS, Incremental Constitutive Laws and their Associated Failure Criteria with Application to Plain Concrete, Int. J. Solids Struct. 8 (1972) 1169-1180

[21] H. KAUDERER, Über ein nichtlineares Elastizitätsgesetz, Ing. Archiv 17 (1949) 450-480

[22] H.B. KUPFER, K.H. GERSTLE, Behaviour of Concrete under Biaxial Stresses, ASCE 99, EM4 (1973) 853-866

[23] K.H. GERSTLE, H. ASCHL et al., Behaviour of Concrete under Multiaxial Stress States, to appear in ASCE ST (1980)

[24] M.D. KOTSOVOS, J.B. NEWMAN, A Model of Concrete Behaviour under Generalised Stress, Proc. IABSE Coll. on Plasticity in Reinforced Concrete, Copenhagen, May 21-23, 1979

[25] B.P. SINHA, K.H. GERSTLE, L.G. TULIN, Stress-Strain Relations for Concrete under Cyclid Loading, ACI J. 61 (1964) 195-210

[26] A.C.T. CHEN, W.-F. CHEN, Constitutive Relations for Concrete, ASCE 101, EM4 (1975) 465-481

[27] J.H. ARGYRIS, G. FAUST, K.J. WILLAM, A Unified Stress-Strain Law for Triaxial Concrete Failure, 3rd Post Conf. on Comput. Aspects of the FEM, Imperial College, London, Sept. 8-9 (1975), G. Davies ed., London, 1975, 359-402

[28] D.W. MURRAY, L. CHITNUYANONDH, K.Y. RIJUB-AGHA, CHUNG WONG, A Concrete Plasticity Theory for Biaxial Stress Analysis, ASCE 105, EM6 (1979) 989-1006

[29] Z.P. BAZANT, P. BHAT, Endochronic Theory of Inelasticity and Failure of Concrete, ASCE 102, EM4 (1976) 701-722

[30] Z.P. BAZANT, Endochronic Inelasticity and Incremental Plasticity, Int. J. Solids Struct. 14 (1978) 691-714

[31] I.S. SANDLER, On the Uniqueness and Stability of Endochronic Theories of Material Behaviour, J. Appl. Mech. 45 (1978) 263-266

[32] Z.P. BAZANT, S.-S. KIM, Plastic-Fracturing Theory of Concrete, ASCE 105, EM3 (1979) 407-428

[33] W.F. CHEN, E.C. TING, Constitutive Models for Concrete Structures, ASCE 106, EM1 (1980) 1-20

[34] J.H. ARGYRIS, L.E. VAZ, K.J. WILLAM, Improved Solution Methods for Inelastic Rate Problems, Comp. Meths. Appl. Mech. Eng. 16 (1978) 231-277

[35] J.H. ARGYRIS, L.E. VAZ, K.J. WILLAM, Integrated Finite Element Analysis of Coupled Thermoviscoplastic Problems, ISD Report No. 283, University of Stuttgart (1980)

[36] H. MATTIES, G. STRANG, The Solution of Nonlinear Finite Element Equations, Int. J. Num. Meth. Eng. 11 (1979) 1613-1626

[37] K.-J. BATHE, A.P. CIMENTO, Some Practical Procedures for the Solution of Nonlinear Finite Element Equations, Comp. Meths. Appl. Mech. Eng. 22 (1980) 59-85

[38] J.H. ARGYRIS, D.W. SCHARPF, Methods of Elasto-Plastic Analysis, Proceed. ISA-ISSC Symp., Stuttgart 1969, 381-416, ZAMP 23 (1972) 517-551

[39] W. PRAGER, Ph. G. HODGE Jr., Theory of Perfectly Plastic Solids, J. Wiley, New York 1951

[40] T.J.R. HUGHES, R.L. TAYLOR, Unconditionally Stable Algorithms for Quasistatic Elasto/Visco-Plastic Finite Element Analysis, Computer & Struct. 8 (1978) 169-173